Supporting Information Figs S1–S9, Tables S1–S5 and Methods S1 & S2

Title: Global variability in leaf respiration in relation to climate, plant functional types and leaf traits

Authors: Owen K. Atkin, Keith J. Bloomfield, Peter B. Reich, Mark G. Tjoelker, Gregory P. Asner, Damien Bonal, Gerhard Bönisch, Matt Bradford, Lucas A. Cernusak, Eric G. Cosio *et al*.

Methods S1 Sampling methods and measurements protocols – unpublished data collected at sites detailed in Table S1.

Species identification

For work undertaken at the RAINFOR plots in South America (http://www.rainfor.org/en/project/field-campaigns), voucher specimens were collected and identified according to Lopez-Gonzalez *et al.* (2011). For South American plots associated with the Carnegie Institution *Spectranomics project* (http://spectranomics.ciw.edu), botanical vouchers were identified as detailed in Asner *et al.* (2014). Species identification at the TERN Supersites (http://www.tern.org.au/Australian-SuperSite-Network-pg17873.html) in Australia were indentified by CSIRO, university and/or forest service botanical staff at each site.

Sampling method (1): Ex situ measurements made using cut branches

Branches being sampled in the morning from the sun-facing upper canopy of individual plants; leaves had experienced at least 2 h direct sunlight before branches were sampled. Branches were recut under water immediately after detachment. Thereafter, branches were transported to a nearby laboratory located for *ex situ* measurements of net CO_2 exchange.

Sampling method (2): In situ measurements using attached branches

Leaf gas exchange measured using attached, sun-facing upper canopy leaves of individual plants, typically between 9:00–13:00 h for most sites, with the exception of measurements in South America, Siberia and Spain, where measurements were made upto 16:00 h.

Measurement methods – leaf gas exchange

(1) Measurements of respiration (R_{dark}) and light-saturated photosynthesis under ambient [CO_2] (A_{sat}) and elevated [CO_2] (A_{max}): most recent, fully expanded leaves were selected for measurement of net CO_2 exchange rates, using Licor 6400 Portable Photosynthesis Systems (Li-6400, LiCor, Lincoln, NE, USA) using a 6 cm^2 leaf chamber with red-blue light source (6400-18 RGB Light Source, Licor). Measurements

were made at a relative humidity (RH) of 60–70%, and at the prevailing ambient daytime T of each site (6–41°C, depending on site location). Leaves were first exposed to saturating irradiance (1000–2000 µmol photons m^{-2} s^{-1}, depending on speices and site) and an reference line atmospheric [CO_2] of 400 ppm for 10 min, after which rates of light-saturated net photosynthesis (A_{sat}) was measured following equilibrium. Thereafter, atmospheric [CO_2] was increased to 1500–2000 ppm (depending on site location), with CO_2-saturated, light-saturated rates of net photosynthesis (A_{max}) then being measured. Finally, which leaves were placed in darkness for 30–45 min (to avoid post-illumination transients; Azcón-Bieto & Osmond, 1983; Atkin et $al.$, 1998) and rates of leaf respiration in darkness (R_{dark}) measured. Flow rates through the leaf chamber were set to 500 and 300 µmol s^{-1} for measurements under light-saturation and darkness, respectively.

(2) Measurements of R_{dark} and A_{sat}: as for (1), but without measurements made at saturating atmospheric [CO_2] (i.e. no estimate of A_{max}).

(3) Measurements of R_{dark} and A_{sat} (from AI curves): as for (1), but with measurements of A_{sat} being limited to measurements made at an atmospheric [CO_2] of 400 ppm (i.e. no estimate of A_{max}) as part of studies of the Kok-effect (Kok, 1948) using light-response curves of net CO_2 exchange (Atkin et $al.$, 2013; Heskel et $al.$, 2014). Measurements commenced at 1800 µmol photons m^{-2} s^{-1} and decreased to 1500, 100 and then at 5 µmol photons m^{-2} s^{-1} intervals to darkness, where R_{dark} was measured. Measurements took place at the prevailing daytime air T at each site (RH 60–70%). An equilibrium period of 2 min was allowed at each irradiance level before net CO_2 exchange was measured. During measurements, CO_2 flow rates in the leaf cuvette were set to 500 µmol s^{-1} for the measurements made at 1800 µmol photons m^{-2} s^{-1} and 300 µmol s^{-1} for those in darkness.

Leaf area, mass and nutrient concentration measurements

At most sites, leaf area was typically determined on a 600 dots inch^{-1} flatbed top-illumination optical scanner, with area being quantified subsequently using *Image J* software (http://imagej.nih.gov/ij/). The scanned leaves were then dried at 70°C for a minimum of 72 h before dry mass (DM) was measured. Leaf mass per area was then calculated as g DM m^2. For sites where both leaf N and P values were reported, concentratons of the two elements were determined with a LaChat QuikChem 8500 Series 2 Flow Injection Analysis System (Lachat Instruments, Milwaukee, WI, USA) using Kjeldahl acid digests (Allen, 1974). For sites where only leaf N was reported, samples were ground using a hammer mill (31–700 Hammer Mill; Glen Creston, Stanmore, UK), weighed into tin cups and combusted using a Carlo-Erba elemental analyser NA1500 (Thermo Fisher Scientific, Milan, Italy).

Methods S2 Temperature normalization of respiration rates.

To enable comparisons of leaf R_{dark}, we calculated rates both for a common temperature (i.e. 25°C) and the estimated growth T at each site (TWQ and MMT). To estimate rates of R_{dark} (R_2) at at given T (T_2), we calculated rates R_{dark} at 25°C (R_{dark}^{25}), TWQ (R_{dark}^{TWQ}) and MMT (R_{dark}^{MMT}) assuming a fixed Q_{10} of 2.23 (Atkin *et al.*, 2005) using the equation:

$$R_2 = R_1 Q_{10}^{\left[\frac{(T_2 - T_1)}{10}\right]} \qquad\qquad \text{Eqn 1}$$

where R_1 represents the rate of R_{dark} at the measurement T (T_1). This approach assumes that the Q_{10} remains constant across a range of leaf T – global surveys of the T-dependence of R_{dark} have shown, however, that the Q_{10} declines with increasing leaf T (Tjoelker *et al.*, 2001; Atkin & Tjoelker, 2003). Given this, we also calculated R_{dark}^{25}, R_{dark}^{TWQ} and R_{dark}^{MMT} using a T-dependent Q_{10} (herein called '*var* Q_{10}')according to:

$$R_2 = R_1 \left(3.09 - 0.043 \left[\frac{(T_2 + T_1)}{2}\right]\right)^{\left[\frac{T_2 - T_1}{10}\right]} \qquad\qquad \text{Eqn 2}$$

Comparison of area-based rates of R_{dark}^{25} calculated using Eqns 1 and 2 revealed little overall difference in predicted rates at 25°C ($r^2 = 0.995$, Fig. S1). Estimates of R_{dark}^{TWQ} were likewise similar, irrespecitive of the equation used ($r^2 = 0.991$, Fig. S1). For subsequent analyses, we used Eqn 2 (i.e. *var* Q_{10}) when estimating rates of R_{dark}^{25}, R_{dark}^{TWQ} and R_{dark}^{MMT}.

Table S1 Details on unpublished databases used in *GlobResp* database of leaf dark respiration (R_{dark})

Country-region	Biome	Latitude	Longitude	Altitude (m a.s.l.)	MAT (°C)	TWQ (°C)	MAP (mm)	PWQ (mm)	AI	No. species	No. measurements	PFTs present	Sampling method (Methods S1)	Measurement method (Methods S2)	Primary person responsible for collection of unpublished data (& senior associate)
USA-AK	Tu	68.630	-149.600	720	-11.3	8.2	225	113	0.608	37	204	BIT, C3H, S	(1)	(3)	N. Mirotchnick (K. Griffin)
Russia-Siberia	BF	62.252	129.621	218	-10.8	15.4	254	122	0.458	3	40	BIT, NIT	(2)	(2)	J. Zaragoza-Castells (O. Atkin)
Russia-Siberia	BF	62.250	129.621	216	-10.8	15.4	254	122	0.458	2	30	BIT, NIT	(2)	(2)	J. Zaragoza-Castells (O. Atkin)
USA-MN	BF	47.944	-91.755	426	3.7	17.3	763	308	0.976	11	182	BIT, NIT	(1)	(2)	P. Reich
USA-MN	BF	46.704	-92.525	385	3.2	17.7	702	288	0.832	7	199	BIT	(1)	(2)	P. Reich
USA-MN	TeDF	45.169	-92.762	210	7.0	21.1	769	315	0.832	1	18	BIT	(1)	(2)	K. Sendall (P. Reich)
USA-NY	TeDF	41.420	-74.010	225	9.4	20.8	1173	308	1.204	3	21	BIT	(1)	(3)	K. Griffin
USA-NY	TeDF	41.420	-74.010	225	9.4	20.8	1173	308	1.204	3	18	BIT	(1)	(3)	K. Griffin
Spain	TeW	40.809	-2.237	980	10.4	18.9	501	102	0.496	1	28	BIT	(2)	(2)	J. Zaragoza-Castells (O. Atkin)
Spain	TeW	40.805	-2.227	1060	11.1	19.6	471	95	0.464	1	24	BIT	(2)	(2)	J. Zaragoza-Castells (O. Atkin)
French Guiana	TrRF_lw	5.270	-52.920	21	25.8	26.2	2824	222	1.881	43	65	BIT	(1)	(1)	J. Zaragoza-Castells (P. Meir)
French Guiana	TrRF_lw	5.270	-52.920	21	25.8	26.2	2824	222	1.881	43	78	BIT	(1)	(1)	J. Zaragoza-Castells (P. Meir)
Peru-Amazon	TrRF_lw	-3.252	-72.908	111	20.6	21.4	2371	676	1.401	20	20	BIT	(1)	(1)	Y. Ishida (J. Lloyd/O. Atkin)
Peru-Amazon	TrRF_lw	-3.256	-72.894	111	26.2	26.7	2821	681	1.667	18	18	BIT	(1)	(1)	Y. Ishida (J. Lloyd/O.Atkin)
Peru-Amazon	TrRF_lw	-3.941	-73.440	120	26.3	26.8	2769	711	1.637	14	14	BIT, S	(1)	(1)	Y. Ishida (J. Lloyd/O.Atkin)
Peru-Amazon	TrRF_lw	-3.949	-73.435	120	26.3	26.8	2769	711	1.638	17	18	BIT	(1)	(1)	Y. Ishida (J. Lloyd/O.Atkin)
Peru-Amazon	TrRF_lw	-3.954	-73.427	120	26.3	26.8	2762	708	1.633	22	22	BIT	(1)	(1)	Y. Ishida (J. Lloyd/O.Atkin)
Peru-Amazon	TrRF_lw	-4.878	-73.630	124	26.7	27.0	2634	618	1.506	14	15	BIT	(1)	(1)	Y. Ishida (J. Lloyd/O.Atkin)
Peru-Amazon	TrRF_lw	-4.899	-73.628	124	26.7	27.0	2639	620	1.506	18	18	BIT	(1)	(1)	Y. Ishida (J. Lloyd/O.Atkin)
Peru-Amazon	TrRF_lw	-12.534	-69.054	200	25.5	26.4	2131	686	1.215	5	5	BIT	(1)	(1)	R. Guerrieri (P. Meir/O.Atkin)
Peru-Amazon	TrRF_lw	-12.830	-69.271	220	25.3	26.3	2477	957	1.436	64	65	BIT	(1)	(1)	J. Zaragoza-Castells & R. Guerrieri
Peru-Amazon	TrRF_lw	-12.831	-69.284	220	25.4	26.3	2491	961	1.445	8	8	BIT	(1)	(1)	R. Guerrieri (P. Meir/O.Atkin)
Peru-Amazon	TrRF_lw	-12.839	-69.296	200	25.4	26.3	2501	964	1.452	71	75	BIT	(1)	(1)	J. Zaragoza-Castells & R. Guerrieri (P. Meir/O.Atkin)
Peru-Andes	TrRF_up	-13.047	-71.542	1750	19.5	20.3	2005	574	1.196	17	20	BIT	(1)	(1)	R. Guerrieri (P. Meir/O.Atkin)
Peru-Andes	TrRF_up	-13.049	-71.537	1500	20.6	21.4	2371	676	1.402	14	16	BIT	(1)	(1)	R. Guerrieri (P. Meir/O.Atkin)
Peru-Andes	TrRF_up	-13.070	-71.556	1800	19.8	20.6	2104	602	1.249	20	20	BIT	(1)	(1)	R. Guerrieri (P. Meir/O.Atkin)
Peru-Andes	TrRF_u	-13.106	-71.589	2750	15.8	16.8	652	188	0.423	10	11	BIT	(1)	(1)	R. Guerrieri (P. Meir/O.Atkin)

Site	Biome	Latitude	Longitude	Elevation	Temp	TWQ	MAP	PWQ	AI	N species	N plants	PFTs			Contributor
Peru-Andes	TrRF_up	-13.109	-71.600	3000	14.2	15.3	359	103	0.244	8	8	BlT	(1)	(1)	R. Guerrieri (P. Meir/O.Atkin)
Peru-Andes	TrRF_up	-13.114	-71.607	3450	11.6	12.8	515	160	0.367	13	14	BlT, C3H	(1)	(1)	R. Guerrieri (P. Meir/O.Atkin)
Peru-Andes	TrRF_up	-13.176	-71.595	3000	13.2	14.3	349	101	0.24	14	16	BlT	(1)	(1)	R. Guerrieri (P. Meir/O.Atkin)
Peru-Andes	TrRF_up	-13.191	-71.588	3000	13.4	14.5	335	97	0.23	7	7	BlT	(1)	(1)	R. Guerrieri (P. Meir/O.Atkin)
Australia-FNQ	TrRF_lw	-17.109	145.603	818	20.5	23.3	1958	886	1.35	6	15	BlT	(1)	(3)	J. Zaragoza-Castells (O. Atkin/P.Meir)
Australia-FNQ	TrRF_lw	-17.120	145.632	728	21.0	23.8	2140	954	1.471	16	56	BlT	(1)	(1)	L. Weerasinghe (O.Atkin)
Australia-FNQ	TrRF_lw	-17.682	145.534	1040	19.0	22.2	1382	641	0.943	10	24	BlT, S	(1)	(3)	J. Zaragoza-Castells(O. Atkin/P.Meir)
Australia-WA	TeW	-30.180	115.000	90	19.0	23.9	558	33	0.386	8	31	BlT, C3H, S	(2)	(1)	L. Weerasinghe (O. Atkin)
Australia-WA	TeW	-30.240	115.070	23	18.8	23.8	558	35	0.389	10	39	BlT, S	(2)	(1)	L. Weerasinghe (O. Atkin)
Australia-WA	TeW	-30.240	115.060	5	18.8	23.8	558	35	0.389	9	34	BlT, C3H, S	(2)	(1)	L. Weerasinghe (O. Atkin)
Australia-WA	TeW	-30.264	120.692	459	18.5	25.6	273	64	0.177	9	87	BlT, S	(1), (2)	(1)	K. Bloomfield (O. Atkin)
Australia-SA	TeW	-34.037	140.674	35	17.3	23.6	255	52	0.172	10	78	BlT, C3H, S	(1), (2)	(1)	K. Bloomfield (O. Atkin)
Australia-ACT	TeW	-35.276	149.109	601	13.1	19.8	637	162	0.509	5	18	BlT, S	(1), (2)	(3)	K. Crous (O. Atkin)
Australia-TAS	TeRF	-43.089	146.651	217	10.1	13.8	1474	237	1.813	3	13	BlT	(1)	(1)	L. Weerasinghe (O. Atkin)
Australia-TAS	TeRF	-43.092	146.684	257	11.2	14.8	1338	212	1.648	2	6	BlT, S	(1)	(1)	L. Weerasinghe (O. Atkin)
Australia-TAS	TeRF	-43.095	146.724	88	11.4	15.1	1255	199	1.463	9	29	BlT, S	(1)	(1)	L. Weerasinghe (O. Atkin)

Shown are individual sample sites, climate and measurement conditions of the sites at which R_{dark} was measured. Sites shown in order from decreasing latitude from north to south. Data on climate are from the *WorldClim* data base (Hijmans *et al.*, 2005). Number of species, plants measured and *JULES* plant functional types (PFTs) at each site shown, according to: BlT, broad-leaved tree; C3H, C_3 metabolism herb/grass; C4H, C_4 metabolism herb/grass; NlT, needle-leaved tree; S, shrub. Biome classes: BF, boreal forests; TeDF, temperate deciduous forest; TeG, temperate grassland; TeRF, temperate rainforest; TeW, temperate woodland; TrRF_lw, lowland tropical rainforest (<1500 m above sea level; a.s.l); TrRF_up, upland tropical rainforest (>1500 m a.s.l); Tu, tundra. TWQ, mean temperature of the warmest quarter (i.e. warmest 3-month period yr^{-1}); MAP, mean annual precipitation; PWQ, mean precipitation of the warmest quarter ; AI, aridity index, calculated as the ratio of MAP to mean annual potential evapotranspiration (UNEP, 1997; Zomer *et al.*, 2008). Australia-ACT, Australian Capital Territory; Australia-FNQ, Far North Queensland; Australia-TAS, Tasmania; Australia-WA, Western Australia; USA-AK, Alaska; USA-MN, Minnesota; USA-NY, New York. See Methods S1 for details on sampling methods and measurement protocols.

Table S2 Details on published databases used in *GlobResp* database of leaf dark respiration (R_{dark})

Country-region	Biome	Latitude	Longitude	Altitude (m a.s.l)	MAT (°C)	TWQ (°C)	MAP (mm)	PWQ (mm)	AI	No. species	PFTs present	Traits available in *GlobResp* database	References/source
Germany	TeDF	50.600	8.700	60	9.1	17.2	704	190	0.917	9	BlT, NlT	R_{dark}, [N], M_a	Grueters (1998); Kattge *et al.* (2011)
USA-MN	BF	47.803	-95.007	400	3.3	18.3	599	278	0.749	1	NlT	R_{dark}, [N]	Tjoelker *et al.* (2008)
USA-MN	BF	46.721	-92.457	380	3.8	17.4	757	304	0.906	7	BlT	R_{dark}, [N]	Machado & Reich (2006)
USA-MN	BF	46.705	-92.525	380	3.7	17.4	764	308	0.905	7	BlT, NlT	R_{dark}, [N]	Reich *et al.* (2008); Tjoelker *et al.* (2008)
USA-MN	TeG	45.410	-93.210	300	6.3	20.4	749	314	0.835	35	BlT, C3H, C4H, S	A_{sat}, C_i, R_{dark}, [N], M_a	Craine *et al.* (1999); Tjoelker *et al.* (2005)
USA-MN	TeDF	45.410	-93.210	300	6.3	20.4	749	314	0.835	3	BlT	A_{sat}, C_i, R_{dark}, M_a	Tjoelker *et al.* (2005); Sendall & Reich (2013)
USA-MN	TeDF	44.996	-93.189	281	7.0	21.0	755	314	0.835	3	BlT	R_{dark}, [N], M_a	Lee *et al.* (2005); Kattge *et al.* (2011)
USA-WI	TeDF	42.980	-90.120	360	7.1	20.2	865	315	0.932	1	BlT	A_{sat}, R_{dark}, [N], M_a	Reich *et al.* (1998b)
USA-MI	TeDF	42.530	-85.855	200	8.6	19.9	944	268	0.98	1	NlT	R_{dark}, [N]	Reich *et al.* (2008); Tjoelker *et al.* (2008)
USA-WI	TeG	42.500	-90.000	275	7.8	20.7	884	315	0.925	15	BlT, C3H, NlT	A_{sat}, C_i, R_{dark}, [N], M_a	Reich *et al.* (1998a,b)
USA-IA	TeDF	41.170	-92.870	385	7.1	20.2	865	315	0.834	11	BlT, NlT	R_{dark}, [N], M_a	Lusk & Reich (2000)
USA-PA	TeDF	40.82	-77.93	400	9.1	17.2	704	190	0.71	1	BlT	A_{sat}, R_{dark}, M_a	Kloeppel *et al.* (1993, 1994)
USA-PA	TeDF	40.8	-77.83	335	9.6	20.8	984	286	0.972	2	BlT	A_{sat}, C_i, R_{dark}, [N], M_a	Kloeppel & Abrams (1995)
USA-PA	TeDF	40.78	-77.88	348	9.5	20.6	986	285	0.986	1	BlT	A_{sat}, C_i, R_{dark}, [N], M_a	Kloeppel & Abrams (1995)
USA-CO	Tu	40.050	-105.600	3360	-2.6	7.5	811	203	1.198	10	BlT, C3H, NlT, S	A_{sat}, C_i, R_{dark}, [N], M_a	Reich *et al.* (1998b)
Japan	TeDF	35.720	140.800	20	14.9	23.7	1619	433	1.921	4	BlT	A_{sat}, R_{dark}, [N], M_a	Miyazawa *et al.* (1998)
USA-TN	TeDF	35.500	-83.500	775	11.2	20.1	1554	389	1.335	13	BlT, C3H, NlT, S	A_{sat}, R_{dark}, [N], M_a	Bolstad *et al.* (1999)
USA-NC	TeDF	35.050	-83.420	850	11.4	20.0	1852	444	1.521	15	BlT, NlT	R_{dark}, [N], M_a	Reich *et al.* (1998b); Mitchell *et al.* (1999)
USA-NM	Sa	34.000	-107.000	1620	12.5	22.2	275	127	0.189	9	BlT, NlT, S	A_{sat}, C_i, R_{dark}, [N], M_a	Reich *et al.* (1998b)
USA-SC	TeDF	33.330	-79.220	3	17.7	25.8	1339	469	1.02	10	BlT, C3H, NlT, S	R_{dark}, [N], M_a	Reich *et al.* (1998a, 1999)
Bangladesh	TrRF_lw	24.200	90.150	21	25.5	28.5	1970	736	1.344	1	BlT	A_{sat}, R_{dark}, M_a	Kamaluddin & Grace (1993)
Niger	Sa	13.200	-2.230	280	28.2	31.4	618	55	0.304	3	BlT, S	A_{sat}, R_{dark}	Meir *et al.* (2007)
Costa Rica	TrRF_lw	10.470	-84.030	140	25.6	26.6	4168	750	2.658	1	BlT	A_{sat}, C_i, R_{dark}, M_a	Oberbauer & Strain (1985); (1986)
Costa Rica	TrRF_lw	10.430	-83.980	105	26.1	27.2	3981	731	2.515	1	S	A_{sat}, R_{dark}, [N], M_a	Chazdon & Kaufmann (1993)
Panama	TrRF_lw	9.170	-79.850	90	26.6	27.5	2624	410	1.877	1	BlT	A_{sat}, C_i, R_{dark}, [N], M_a	Zotz & Winter (1996)
Panama	TrRF_lw	8.983	-79.550	100	27.0	27.7	1820	300	1.186	13	BlT	A_{sat}, C_i, R_{dark}, [N], [P], M_a	Slot *et al.* (2014)
Panama	TrRF_lw	8.970	-79.530	30	27.1	27.7	1762	290	1.143	6	BlT	A_{sat}, C_i, R_{dark}, [N], M_a	Kitajima *et al.* (1997)
Venezuela	TrRF_lw	8.650	-71.400	2350	14.7	15.1	1400	458	1.053	1	BlT	A_{sat}, C_i, R_{dark}, [N], M_a	García-Núñez *et al.*(1995)

Location	Type	Lat	Lon	Elev						N	Codes	Variables	Reference
Malaysia	TrRF_lw	5.160	117.900	20	26.7	27.1	2471	501	1.638	29	Malaysia-Borneo	A_{sat}, C_i, R_{dark}, [N], [P], M_a	Swaine (2007)
Cameroon	TrRF_lw	3.380	11.500	550	24.0	24.8	1729	417	1.126	6	Cameroon	A_{sat}, R_{dark}, [N], M_a	Meir *et al.* (2007)
Suriname	TrRF_lw	2.854	-54.958	215	25.4	26.3	2224	165	1.365	25	Suriname	A_{sat}, R_{dark}, [N], M_a	Kattge *et al.* (2011)
Venezuela	TrRF_lw	1.930	-67.050	120	26.3	26.6	3430	740	1.725	9	Venezuela	A_{sat}, C_i, R_{dark}, [N], M_a	Reich *et al.* (1998b)
Brazil-Amazon	TrRF_lw	-2.580	-60.100	115	27.0	27.6	2232	401	1.385	9	BlT	R_{dark}, [N], M_a	Meir *et al.* (2002)
Bolivia	TrRF_lw	-15.783	-62.917	400	25.3	27.0	1020	436	0.57	50	BlT	A_{sat}, R_{dark}, [N], M_a	Poorter & Bongers (2006)
Australia-FNQ	TrRF_lw	-16.100	145.450	90	25.2	27.5	2087	1031	1.393	18	BlT	A_{sat}, C_i, R_{dark}, [N], [P], M_a	Weerasinghe *et al.* (2014)
Australia-WA	TeW	-31.500	115.690	15	18.4	23.6	728	39	0.541	25	BlT, C3H, S	A_{sat}, C_i, R_{dark}, [N], M_a	Wright *et al.* (2004)
South Africa	TeW	-33.830	18.830	600	16.6	21.0	754	67	0.572	5	BlT, S	A_{sat}, R_{dark}, [N], M_a	Mooney *et al.* (1983)
Australia-NSW	TeW	-33.840	145.880	223	17.0	24.2	422	98	0.294	19	BlT, C3H, NlT, S	A_{sat}, C_i, R_{dark}, [N], [P], M_a	Wright *et al.* (2001)
Australia-NSW	TeW	-33.840	145.880	223	17.0	24.2	422	98	0.294	21	BlT, C4H, S	A_{sat}, C_i, R_{dark}, [N], [P], M_a	Wright *et al.* (2001)
Australia-NSW	TeW	-33.860	151.210	39	17.6	21.9	1309	358	NA	18	BlT, S	A_{sat}, C_i, R_{dark}, [N], [P], M_a	Wright *et al.* (2001)
Australia-NSW	TeW	-33.860	151.210	39	17.6	21.9	1309	358	NA	17	BlT, S	A_{sat}, C_i, R_{dark}, [N], [P], M_a	Wright *et al.* (2001)
Australia-ACT	TeW	-35.312	149.058	560	13.0	21.0	755	314	0.601	1	NlT	A_{sat}, C_i, R_{dark}, [N], M_a	Reich *et al.* (1999))
Chile	TeRF	-36.840	-73.030	30	12.2	16.1	1272	74	1.208	6	BlT	A_{sat}, C_i, R_{dark}, [N], M_a	Wright *et al.* (2006)
Chile	TeRF	-37.000	-71.470	1000	6.2	11.5	1189	74	1.119	5	BlT, NlT	A_{sat}, C_i, R_{dark}, [N], M_a	Wright *et al.* (2006)
Chile	TeRF	-39.800	-73.000	400	12.5	16.7	1680	129	1.622	12	BlT	A_{sat}, C_i, R_{dark}, [N], M_a	Wright *et al.* (2006)
New Zealand	TeRF	-43.250	170.180	68	11.9	16.3	4331	1103	4.866	3	BlT, NlT	A_{sat}, C_i, R_{dark}, [N], [P], M_a	Atkin *et al.* (2013)
New Zealand	TeRF	-43.310	170.170	143	11.2	15.8	4277	1076	4.816	3	BlT, NlT	A_{sat}, C_i, R_{dark}, [N], [P], M_a	Atkin *et al.* (2013)
New Zealand	TeRF	-43.380	170.180	134	11.6	16.2	4017	1017	4.468	3	BlT	A_{sat}, C_i, R_{dark}, [N], [P], M_a	Atkin *et al.* (2013)
New Zealand	TeRF	-43.400	170.170	234	11.4	16.0	3980	1004	4.477	7	BlT	A_{sat}, C_i, R_{dark}, [N], [P], M_a	Atkin *et al.* (2013)
New Zealand	TeRF	-43.410	170.170	271	10.9	15.6	3920	980	4.409	6	BlT, S	A_{sat}, C_i, R_{dark}, [N], [P], M_a	Atkin *et al.* (2013)
New Zealand	TeRF	-43.420	170.170	215	11.2	15.8	3883	976	4.343	5	BlT, S	A_{sat}, C_i, R_{dark}, [N], [P], M_a	Atkin *et al.* (2013)

Shown are climate and measurement conditions of the sites at which R_{dark} was measured. Sites shown in order from decreasing latitude from north to south. Data on climate are from the *WorldClim* data base (Hijmans *et al.*, 2005). Number of species and *JULES* plant functional types (PFTs) at each site shown, according to: BlT, broad-leaved tree; C3H, C_3 metabolism herb/grass; C4H, C_4 metabolism herb/grass; NlT, needle-leaved tree; S, shrub. Biome classes: BF, boreal forests; TeDF, temperate deciduous forest; TeG, temperate grassland; TeRF, temperate rainforest; TeW, temperate woodland; TrRF_lw, lowland tropical rainforest (<1500 m above sea level; a.s.l.); Tu, tundra. TWQ, mean temperature of the warmest quarter (i.e. warmest 3-month period yr^{-1}); MAP, mean annual precipitation; PWQ, mean precipitation of the warmest quarter; AI, aridity index, calculated as the ratio of MAP to mean annual potential evapotranspiration (UNEP, 1997; Zomer *et al.*, 2008). NA, not applicable. Australia-ACT, Australian Capital Territory; Australia-FNQ, Far North Queensland; Australia-NSW, New South Wales; Australia-WA, Western Australia; USA-AK, Alaska; USA-CO, Colorado; USA-MN, Minnesota; USA-IW, Iowa; USA-WI, Wisconsin; USA-MI, Michigan; USA-PN, Pennsylvania; USA-NC, North Carolina; USA-KT, Kentucky; USA-TN, Tennessee; USA-NM, New Mexico; USA-SC, South Carolina.

Table S3 Standardized major axis regression slopes and their confidence intervals for log–log transformed relationships shown in Figs 5 and 6

Fig.	Response	Bivariate	JULES PFTs	H0 No. 1: no difference in slope (P-value)	PFT or TWQ-class (°C)	n	r^2	P	Slope	Pairwise comparison	Slope CI_low	Slope CI_high	Intercept	H0 No. 2: no difference in elevation (P-value)	Intercepts for a common slope	Pairwise comparison (where relationship significant)	H0 No. 3: no difference in 'shift'.p-value
5(a)	$R_{dark,a}^{25}$	$V_{cmax,a}^{25}$	All bar C4H	0.7017	BIT	691	0.12	<0.0001	0.976		0.910	1.046	-1.445	<0.0001	-1.470	*a*	< 0.0001
					C3H	45	0.00	*0.8940*	1.073		0.793	1.453	-1.414		-1.279		
					NIT	23	0.16	*0.0578*	0.949		0.633	1.422	-1.445		-1.510		
					S	115	0.16	< 0.0001	1.076		0.908	1.276	-1.647		-1.501	*a*	
5 (d)	$R_{dark,m}^{25}$	$V_{cmax,m}^{25}$	All bar C4H	<0.0001	BIT	682	0.27	<0.0001	0.946	b	0.887	1.009	-1.351				
					C3H	44	0.37	<0.0001	1.247	a	0.977	1.592	-1.962				
					NIT	23	0.62	<0.0001	0.494	c	0.375	0.651	-0.366				
					S	115	0.31	<0.0001	1.057	a, b	0.906	1.234	-1.671				
5(b)	$R_{dark,a}^{25}$	$V_{cmax,a}^{25}$	All bar C4H	0.0857	<10	47	0.19	0.0023	1.273		0.974	1.662	-1.592	<0.0001	-1.134	*d*	<0.0001
					10–15	43	0.18	0.0042	1.103		0.832	1.461	-1.484		-1.287	*c*	
					15–20	121	0.33	<0.0001	0.849		0.732	0.985	-1.270		-1.476	*a, b*	
					20–25	263	0.30	<0.0001	0.966		0.872	1.069	-1.487		-1.507	*a*	
					>25	400	0.03	0.0004	0.999		0.907	1.101	-1.475		-1.445	*b*	
5(e)	$R_{dark,m}^{25}$	$V_{cmax,m}^{25}$	All bar C4H	<0.0001	<10	47	0.62	<0.0001	1.093	a	0.909	1.314	-1.412				
					10–15	42	0.38	<0.0001	1.165	a	0.908	1.496	-1.720				
					15–20	121	0.68	<0.0001	0.752	b	0.679	0.832	-0.875				
					20–25	258	0.31	<0.0001	0.920	a	0.831	1.019	-1.356				
					>25	396	0.15	<0.0001	1.002	a	0.914	1.098	-1.482				
5(c)	$R_{dark,a}^{25}$	$V_{cmax,a}^{25}$	BIT only	0.0480	<10	4	0.63	*0.2070*	-2.446		-9.686	-0.618	4.306	<0.0001	-1.061		<0.0001
					10–15	39	0.21	0.0036	1.033		0.771	1.384	-1.352		-1.204	*c*	
					15–20	101	0.35	<0.0001	0.805		0.685	0.945	-1.183		-1.401	*b*	
					20–25	152	0.17	<0.0001	0.865		0.747	1.001	-1.325		-1.440	*a*	
					>25	395	0.03	0.0006	1.011		0.917	1.115	-1.494		-1.391	*b*	
5(f)	$R_{dark,m}^{25}$	$V_{cmax,a}^{25}$	BIT only	<0.0001	<10	4	0.41	*0.3627*	8.035		1.642	39.317	-20.639				
					10–15	39	0.40	<0.0001	1.103	a	0.855	1.423	-1.549				
					15–20	101	0.72	<0.0001	0.753	b	0.678	0.836	-0.862				
					20–25	147	0.15	<0.0001	0.821	b	0.706	0.955	-1.109				
					>25	391	0.13	<0.0001	1.022	a	0.932	1.121	-1.533				
6(a)	$R_{dark,a}^{25}$	Leaf [N]a	All bar C4H	0.5081	BIT	794	0.10	<0.0001	1.134		1.061	1.211	-0.296	<0.0001	-0.300	*a*	<0.0001
					C3H	74	0.30	<0.0001	1.169		0.961	1.421	-0.071		-0.065	*c*	
					NIT	30	0.32	0.0010	1.005		0.735	1.375	-0.287		-0.346	*a*	
					S	132	0.26	<0.0001	1.257		1.084	1.458	-0.215		-0.180	*b*	
6(d)	$R_{dark,m}^{25}$	Leaf [N]m	All bar C4H	0.0093	BIT	805	0.11	<0.0001	1.423	a	1.333	1.519	-0.781				
					C3H	74	0.60	<0.0001	1.598	a	1.379	1.852	-0.818				
					NIT	39	0.09	*0.0576*	2.354		1.723	3.217	-1.763				
					S	132	0.43	<0.0001	1.383	a	1.213	1.576	-0.579				
6 (b)	$R_{dark,a}^{25}$	Leaf [N]a	All bar C4H	0.0512	<10	47	0.14	0.0109	1.224	a, b	0.929	1.613	-0.008	<0.0001	0.025	*a*	<0.0001
					10–15	37	0.15	0.0170	1.700	a	1.245	2.320	-0.399		-0.187	*b,c*	
					15–20	92	0.25	<0.0001	1.170	b	0.976	1.401	-0.198		-0.185	*b*	
					20–25	345	0.29	<0.0001	1.141	b	1.043	1.248	-0.256		-0.251	*c*	
					>25	509	0.04	<0.0001	1.056	b	0.969	1.150	-0.301		-0.316	*d*	
6(e)	$R_{dark,m}^{25}$	Leaf [N]m	All bar C4H	0.0005	<10	47	0.60	<0.0001	1.821	a	1.508	2.198	-1.056				
					10–15	37	0.44	<0.0001	2.040	a	1.583	2.629	-1.415				
					15–20	108	0.44	<0.0001	1.695	a, b	1.468	1.956	-0.941				
					20–25	350	0.36	<0.0001	1.451	b, c	1.334	1.579	-0.772				
					>25	508	0.06	<0.0001	1.333	c	1.225	1.451	-0.695				
6(c)	$R_{dark,a}^{25}$	Leaf [N]a	BIT only	0.0004	<10	4	0.90	*0.0537*	10.773		4.514	25.707	-3.357				
					10–15	34	0.10	*0.0714*	1.680		1.201	2.350	-0.389				
					15–20	76	0.20	<0.0001	1.320	a	1.075	1.621	-0.214				
					20–25	186	0.28	<0.0001	1.002	b	0.886	1.133	-0.278				
					>25	494	0.03	<0.0001	1.050	b	0.963	1.146	-0.301				
6(f)	$R_{dark,m}^{25}$	Leaf [N]m	BIT only	0.0041	<10	4	0.97	0.0161	2.677	a	1.591	4.503	-2.491				
					10–15	34	0.38	0.0001	2.140	a	1.616	2.833	-1.547				
					15–20	85	0.44	<0.0001	1.586	a, b	1.347	1.868	-0.799				
					20–25	189	0.26	<0.0001	1.479	b	1.307	1.674	-0.881				

| >25 | 493 | 0.05 | <0.0001 | 1.346 | b | 1.235 | 1.467 | -0.713 |

Coefficients of determination (r^2) and significance values (P) of each bivariate relationship are shown. Ninety-five percent confidence intervals (CI) of SMA slopes and y-axis intercepts are shown in parentheses. In cases where SMA tests for common slopes revealed no significant differences between the upper canopy and lower canopy groups (i.e. $P > 0.05$), when plotting bivariate relationships, common slopes were used (with CI of the common slopes provided). Where there was a significant difference in elevation of the common-slope SMA regressions, values for the y-axis intercept (elevation) are provided. Where appropriate, significant shifts along a common slopes are indicated. *JULES* PFTs: BlT, broad-leaved tree; C3H, C_3 metabolism herb/grass; C4H, C_4 metabolism herb/grass; NlT, needle-leaved tree; S, shrub. TWQ classes: <10°C; 10–15°C; 15–20°C; 20–25°C; >25°C. $R_{dark,a}^{25}$, predicted area-based R_{dark} at 25°C; $R_{dark,m}^{25}$, mass-based R_{dark} at 25°C; $V_{cmax,a}^{25}$, predicted area-based V_{cmax} at 25°C; $V_{cmax,m}^{25}$, predicted mass-based V_{cmax} at 25°C.

Table S4 Comparison of linear mixed-effects models with area-based leaf respiration at 25°C ($R_{\text{dark,a}}^{25}$; μmol CO_2 m^{-2} s^{-1}) as the response variable (each showing fixed and random effects), with input data restricted to site : species means for which all potential fixed effect parameters were available

Table S4

Fixed effect	Best predictor model Estimate	S.E.	t value	Null model (PFT only) Estimate	S.E.	t value	ESM #1 Estimate	S.E.	t value	ESM #2 Estimate	S.E.	t value	ESM #3 Estimate	S.E.	t value	ESM #4 Estimate	S.E.	t value
PFT_JULES_BIT (if other variables were at global mean)	1.2636	0.033	38.551	1.3805	0.046	29.750	1.2704	0.011	119.349	1.3000	0.012	105.939	1.2855	0.011	117.099	1.2618	0.011	118.611
PFT_JULES_C3H	0.4708	0.141	3.348	0.5099	0.160	3.185	0.3591	0.027	13.135	0.3642	0.030	12.232	0.4395	0.028	15.657	0.4120	0.027	15.176
PFT_JULES_NIT	-0.3595	0.150	-2.392	-0.0558	0.179	-0.311	0.0657	0.033	1.989	-0.0272	0.036	-0.748	-0.2566	0.036	-7.175	0.0259	0.033	0.782
PFT_JULES_S	0.3290	0.064	5.163	0.3460	0.071	4.867	0.3028	0.015	20.290	0.2873	0.016	17.704	0.3188	0.015	20.655	0.3141	0.015	21.009
Leaf [N] (units vary with model, see note below)	0.0728	0.018	4.124				0.0075	0.001	12.574	0.0104	0.001	16.077	0.2061	0.004	46.314			
Leaf_Pa	0.0015	0.000	7.389															
Vcmax_a_25	0.0095	0.001	15.241				0.0114	0.000	58.237							0.0116	0.000	59.229
MeanT.Warmest.Qtr	-0.0358	0.006	-5.658				-0.0338	0.002	-17.949	-0.0389	0.002	-17.983	-0.0402	0.002	-21.055	-0.0334	0.002	-17.766
PFT_JULES_C3H : Leaf_Na	0.3394	0.069	4.892															
PFT_JULES_NIT : Leaf_Na	0.0762	0.146	0.523															
PFT_JULES_S : Leaf_Na	0.0687	0.053	1.295															

Random effect	No. levels per group	Variance compone	% of total	Variance compone	% of total	No. levels per group	Variance compone	% of total	Variance compone	% of total	Variance compone	% of total	Variance compone	% of total
Intercept variance: Among species	531	0.009	7.1%	0.023	11.5%	655	0.000	0.0%	0.000	0.0%	0.000	1.9%	0.000	0.0%
Intercept variance: Among families	100	0.002	1.4%	0.004	2.1%	114	0.000	2.4%	0.001	3.0%	0.001	4.5%	0.000	2.6%
Intercept variance: Among sites	49	0.031	23.4%	0.073	36.2%	64	0.005	32.8%	0.006	36.6%	0.005	31.1%	0.005	32.5%
Residual (within species, families and sites plus real error)		0.091	68.2%	0.102	50.2%		0.009	64.8%	0.010	60.5%	0.009	62.4%	0.009	64.9%
		0.133	100.0%	0.202	100.0%		0.014	100.0%	0.017	100.0%	0.015	100.0%	0.014	100.0%
Likelihood ratio test		-595.2		-681.9			-633.7		-689.7		-653.1		-631.9	
Akaike (AIC)		1,220		1,380			1,289		1,399		1,326		1,284	
Bayesian (BIC)		1,288		1,416			1,341		1,446		1,373		1,331	
REML criterion at convergence		1,190		1,364			1,267		1,379		1,306		1,264	
Number of observations (Site:Spp averaged)	667					802								

Continuous explanatory variables HAVE been centred on their means.
Leaf N is included on an AREA basis in models: Best, Null and ESM 3. And on a MASS basis in ESM 1 and 2.
The Best and Null models are run on a smaller subset of data given the requirement for Leaf P values.

Several model frameworks are outlined (a 'best predictor model, followed by a null model using PFTs only as fixed factors, then models relevant to different model frameworks, here called 'ESM' frameworks), each containing different combinations of fixed effect parameter values (ESM No. 1–4; for details of each framework, see below). For the fixed effects subtable, parameter values, SE and *t*-values given for the continuous explanatory variables; explanatory variables (all centred on their means) are: 1, plant functional types (PFT), according to *JULES* (Clark *et al.*, 2011): BlT, broad-leaved tree; C3H, C_3 metabolism herbs/grasses; NlT, needle-leaved trees; S, shrubs; 2, area-based or mass-based leaf nitrogen [N_a (g m^{-2}) or N_m (mg g^{-1}), respectively] area-based phosphorus (P_a; g m^{-2}) concentrations, area-based Rubisco CO_2 fixation capacity at 25°C ($V_{\text{cmax,a}}^{25}$; μmol CO_2 m^{-2} s^{-1}), and mean temperature of the warmest quarter (TWQ; °C) (Hijmans *et al.*, 2005). The PFT-BlT values (first row) are based on the assumption that other variables were at their global mean values. In the 'best' model (i.e. same as that shown in Table 5 and Fig. 9), all available and relevant parameters were included in model selection (PFTs, $V_{\text{cmax,a}}^{25}$, N_a, P_a, TWQ, precipitation of the warmest quarter (PWQ) and aridity index (AI)). The null model provides a model where fixed effect factor is limited to PFTs. For ESM#1, the model was limited to the following source fixed effect parameters: PFT, N_m and $V_{\text{cmax,a}}^{25}$ and TWQ. Here, our decision to include mass-based N was based on the fact that mass-based N is a predictive trait used in *JULES*, according to Schulze *et al.* (1994). For ESM#2, source fixed effect parameters were the same as for ESM#1, but without $V_{\text{cmax,a}}^{25}$. For ESM#3, input fixed effect parameters were: PFT, N_a and TWQ, while for ESM#4, they were PFT, $V_{\text{cmax,a}}^{25}$ and TWQ. In the random effect subtable, the intercept was allowed to vary among species, families and sites; residual errors shown are within species, families, sites and investigators. Finally, predictive equations are shown that enable $R_{\text{dark,a}}^{25}$ to be predicted based on inputs according to the six models (see next page).

Table S4 Continued

Best predictor model (from Table 6)
Broad-leaved trees: $R_{\text{dark,a}}^{25} = 1.236 + (0.0728 \times [\text{N}]_a) + (0.015 \times [\text{P}]_a) + (0.0095 \times V_{\text{cmax,a}}^{25}) - (0.0358 \times \text{TWQ})$
C$_3$ herbs/grasses: $R_{\text{dark,a}}^{25} = 1.7344 + (0.4122 \times [\text{N}]_a) + (0.015 \times [\text{P}]_a) + (0.0095 \times V_{\text{cmax,a}}^{25}) - (0.0358 \times \text{TWQ})$
Needle-leaved trees: $R_{\text{dark,a}}^{25} = 0.9041 + (0.1489 \times [\text{N}]_a) + (0.015 \times [\text{P}]_a) + (0.0095 \times V_{\text{cmax,a}}^{25}) - (0.0358 \times \text{TWQ})$
Shrubs: $R_{\text{dark,a}}^{25} = 1.5926 + (0.1415 \times [\text{N}]_a) + (0.015 \times [\text{P}]_a) + (0.0095 \times V_{\text{cmax,a}}^{25}) - (0.0358 \times \text{TWQ})$

Null model (PFT only) (from Table 6)
Broad-leaved trees: $R_{\text{dark,a}}^{25} = 1.3805$
C$_3$ herbs/grasses: $R_{\text{dark,a}}^{25} = 1.8904$
Needle-leaved trees: $R_{\text{dark,a}}^{25} = 1.3247$
Shrubs: $R_{\text{dark,a}}^{25} = 1.7265$

ESM#1
Broad-leaved trees: $R_{\text{dark,a}}^{25} = 1.2704 + (0.0075 \times [\text{N}]_m) + (0.0114 \times V_{\text{cmax,a}}^{25}) - (0.0338 \times \text{TWQ})$
C$_3$ herbs/grasses: $R_{\text{dark,a}}^{25} = 1.6295 + (0.0075 \times [\text{N}]_m) + (0.0114 \times V_{\text{cmax,a}}^{25}) - (0.0338 \times \text{TWQ})$
Needle-leaved trees: $R_{\text{dark,a}}^{25} = 1.3361 + (0.0075 \times [\text{N}]_m) + (0.0114 \times V_{\text{cmax,a}}^{25}) - (0.0338 \times \text{TWQ})$
Shrubs: $R_{\text{dark,a}}^{25} = 1.5732 + (0.0075 \times [\text{N}]_m) + (0.0114 \times V_{\text{cmax,a}}^{25}) - (0.0338 \times \text{TWQ})$

ESM#2
Broad-leaved trees: $R_{\text{dark,a}}^{25} = 1.300 + (0.0104 \times [\text{N}]_m) - (0.0389 \times \text{TWQ})$
C$_3$ herbs/grasses: $R_{\text{dark,a}}^{25} = 1.66642 + (0.0104 \times [\text{N}]_m) - (0.0389 \times \text{TWQ})$
Needle-leaved trees: $R_{\text{dark,a}}^{25} = 1.2728 + (0.0104 \times [\text{N}]_m) - (0.0389 \times \text{TWQ})$
Shrubs: $R_{\text{dark,a}}^{25} = 1.5875 + (0.0104 \times [\text{N}]_m) - (0.0389 \times \text{TWQ})\text{TWQ})$

ESM#3
Broad-leaved trees: $R_{\text{dark,a}}^{25} = 1.2855 + (0.2061 \times [\text{N}]_a) - (0.0402 \times \text{TWQ})$
C$_3$ herbs/grasses: $R_{\text{dark,a}}^{25} = 1.7250 + (0.2061 \times [\text{N}]_a) - (0.0402 \times \text{TWQ})$
Needle-leaved trees: $R_{\text{dark,a}}^{25} = 1.0290 + (0.2061 \times [\text{N}]_a) - (0.0402 \times \text{TWQ})$
Shrubs: $R_{\text{dark,a}}^{25} = 1.6043 + (0.2061 \times [\text{N}]_a) - (0.0402 \times \text{TWQ})$

ESM#4
Broad-leaved trees: $R_{\text{dark,a}}^{25} = 1.2818 + (0.0116 \times V_{\text{cmax,a}}^{25}) - (0.0334 \times \text{TWQ})$
C$_3$ herbs/grasses: $R_{\text{dark,a}}^{25} = 1.6737 + (0.0116 \times V_{\text{cmax,a}}^{25}) - (0.0334 \times \text{TWQ})$
Needle-leaved trees: $R_{\text{dark,a}}^{25} = 1.2877 + (0.0116 \times V_{\text{cmax,a}}^{25}) - (0.0334 \times \text{TWQ})$
Shrubs: $R_{\text{dark,a}}^{25} = 1.5758 + (0.0116 \times V_{\text{cmax,a}}^{25}) - (0.0334 \times \text{TWQ})$

Table S5 Comparison of linear mixed-effects models using different plant functional types (PFT) classifications, with leaf respiration at 25°C (R_{dark}^{25}) as the response variable

(a) Area-based

JULES

Fixed effect	Estimate	S.E.	t value
PFT_JULES_BlT (if other variables were at global mean)	1.1911	0.034	35.041
PFT_JULES_C3H	0.3930	0.069	5.709
PFT_JULES_NlT	0.1392	0.091	1.536
PFT_JULES_S	0.3298	0.045	7.298
Leaf [N]_area	0.2589	0.014	18.973
MeanT_Warmest.Qtr	-0.0396	0.006	-6.381

LPJ

Fixed effect	Estimate	S.E.	t value
PFT_LPJ _BorDcBl	1.3667	0.152	8.982
PFT_LPJ_BorDcNl	0.2756	0.166	1.659
PFT_LPJ_BorEvNl	-0.5574	0.234	-2.382
PFT_LPJ_TmpDcBl	-0.1969	0.152	-1.292
PFT_LPJ_TmpEvBl	0.0018	0.149	0.012
PFT_LPJ_TmpEvNl	-0.0581	0.177	-0.329
PFT_LPJ_TmpH	0.1723	0.151	1.141
PFT_LPJ_TrpDcBl	-0.1469	0.167	-0.881
PFT_LPJ_TrpEvBl	-0.1785	0.162	-1.104
PFT_LPJ_TrpH	0.0177	0.267	0.066
Leaf [N]_area	0.2592	0.014	18.407
MeanT_Warmest.Qtr	-0.0351	0.007	-4.743

JULES random effects

Random effect	Variance component	% of total
Intercept variance: Among species	0.000	0.0%
Intercept variance: Among families	0.008	3.4%
Intercept variance: Among sites	0.056	24.1%
Residual (within species, families and sites plus real error)	0.167	72.5%
	0.230	100.0%

logLikelihood	-1,011
Akaike (AIC)	2,041
Bayesian (BIC)	2,091
REML criterion at convergence	2,021

LPJ random effects

Random effect	Variance component	% of total
Intercept variance: Among species	0.000	0.0%
Intercept variance: Among families	0.007	2.8%
Intercept variance: Among sites	0.061	25.7%
Residual (within species, families and sites plus real error)	0.170	71.5%
	0.237	100.0%

logLikelihood	-1,022
Akaike (AIC)	2,075
Bayesian (BIC)	2,154
REML criterion at convergence	2,043

Number of obs: 1025
Groups: Species, 833; Family, 129; Site, 81
Continuous explanatory variables HAVE been centred on their means

(b) Mass-based

JULES

Fixed effect	Estimate	S.E.	t value
PFT_JULES_BlT (if other variables were at global mean)	11.0413	0.068	161.680
PFT_JULES_C3H	4.1153	0.125	32.816
PFT_JULES_NlT	-2.0938	0.156	-13.408
PFT_JULES_S	1.6953	0.073	23.248
Leaf [N]_mass	0.4586	0.003	135.520
MeanT_Warmest.Qtr	-0.3842	0.013	-30.559

LPJ

Fixed effect	Estimate	S.E.	t value
PFT_LPJ _BorDcBl	14.7990	0.254	58.233
PFT_LPJ_BorDcNl	0.7859	0.409	1.921
PFT_LPJ_BorEvNl	-7.7081	0.303	-25.481
PFT_LPJ_TmpDcBl	-2.8388	0.258	-11.000
PFT_LPJ_TmpEvBl	-3.5225	0.250	-14.069
PFT_LPJ_TmpEvNl	-5.7636	0.293	-19.703
PFT_LPJ_TmpH	0.2726	0.257	1.062
PFT_LPJ_TrpDcBl	-3.5374	0.288	-12.268
PFT_LPJ_TrpEvBl	-3.8196	0.275	-13.872
PFT_LPJ_TrpH	-2.3686	0.476	-4.974
Leaf [N]_mass	0.4567	0.003	133.980
MeanT_Warmest.Qtr	-0.3353	0.015	-23.104

JULES random effects

Random effect	Variance component	% of total
Intercept variance: Among species	0.000	0.0%
Intercept variance: Among families	0.036	8.9%
Intercept variance: Among sites	0.258	64.3%
Residual (within species, families and sites plus real error)	0.108	26.9%
	0.401	100.0%

logLikelihood	-2,655
Akaike (AIC)	5,330
Bayesian (BIC)	5,379
REML criterion at convergence	5,310

LPJ random effects

Random effect	Variance component	% of total
Intercept variance: Among species	0.000	0.0%
Intercept variance: Among families	0.033	8.2%
Intercept variance: Among sites	0.262	65.0%
Residual (within species, families and sites plus real error)	0.108	26.8%
	0.403	100.0%

logLikelihood	-2,644
Akaike (AIC)	5,319
Bayesian (BIC)	5,398
REML criterion at convergence	5,287

Response variable is Rdarkm_25C_varQ10
Continuous explanatory variables HAVE been centred on their means
Number of obs: 1045
Groups: Species, 833; Family, 129; Site, 87

Two models are shown: (a) using area-based leaf respiration at 25°C ($R_{\text{dark,a}}^{25}$; µmol CO_2 m^{-2} s^{-1}); and, (b) mass-based leaf respiration at 25°C ($R_{\text{dark,m}}^{25}$; nmol CO_2 g^{-1} s^{-1}). For (a) and (b), two model frameworks are outlined (variants of ESM#3 model shown in Table S4, but with a larger number of observations reflecting the abundance of [N]$_a$ (g m^{-2}) and [N]$_m$ (mg g^{-1}) data), differing in the plant functional types (PFT) used: *JULES*(Clark *et al.*, 2011): BlT, broad-leaved tree; C3H, C_3 metabolism herbs/grasses; NlT, needle-leaved trees; S, shrubs; and, *LPJ* (Sitch *et al.*, 2003): BorDcBl, boreal deciduous broad-leaved tree/shrub; BorDcNl, boreal deciduous needle-leaved tree/shrub; BorEvNl, boreal evergreen needle-leaved tree/shrub; TmpDcBl, temperate deciduous broad-leaved tree/shrub; TmpEvBl, temperate evergreen broad-leaved tree/shrub; TmpEvNl, temperate evergreen needle-leaved tree/shrub; TmpH, temperate herb/grass; TrpDcBl, tropical deciduous broad-leaved tree/shrub; TrpEvBl, tropical evergreen broad-leaved tree/shrub; TrpH, tropical herb/grass. For the fixed effects subtables, parameter values, SE and *t*-values given for the continuous explanatory variables; explanatory variables (all centred on their means) are: PFTs; area or mass-based leaf nitrogen (N$_a$ and N$_m$, respectively) and mean temperature of the warmest quarter (TWQ) (Hijmans *et al.*, 2005). For *JULES*, the

PFT-BlT values (first row) are based on the assumption that other variables were at their global mean values. Similarly, for *LPJ*, the PFT-BorDcBl (first row) are based on the assumption that other variables were at their global mean values. In the random effect subtable, the intercept was allowed to vary among species, families and sites; residual errors shown are within species, families, sites and investigators.
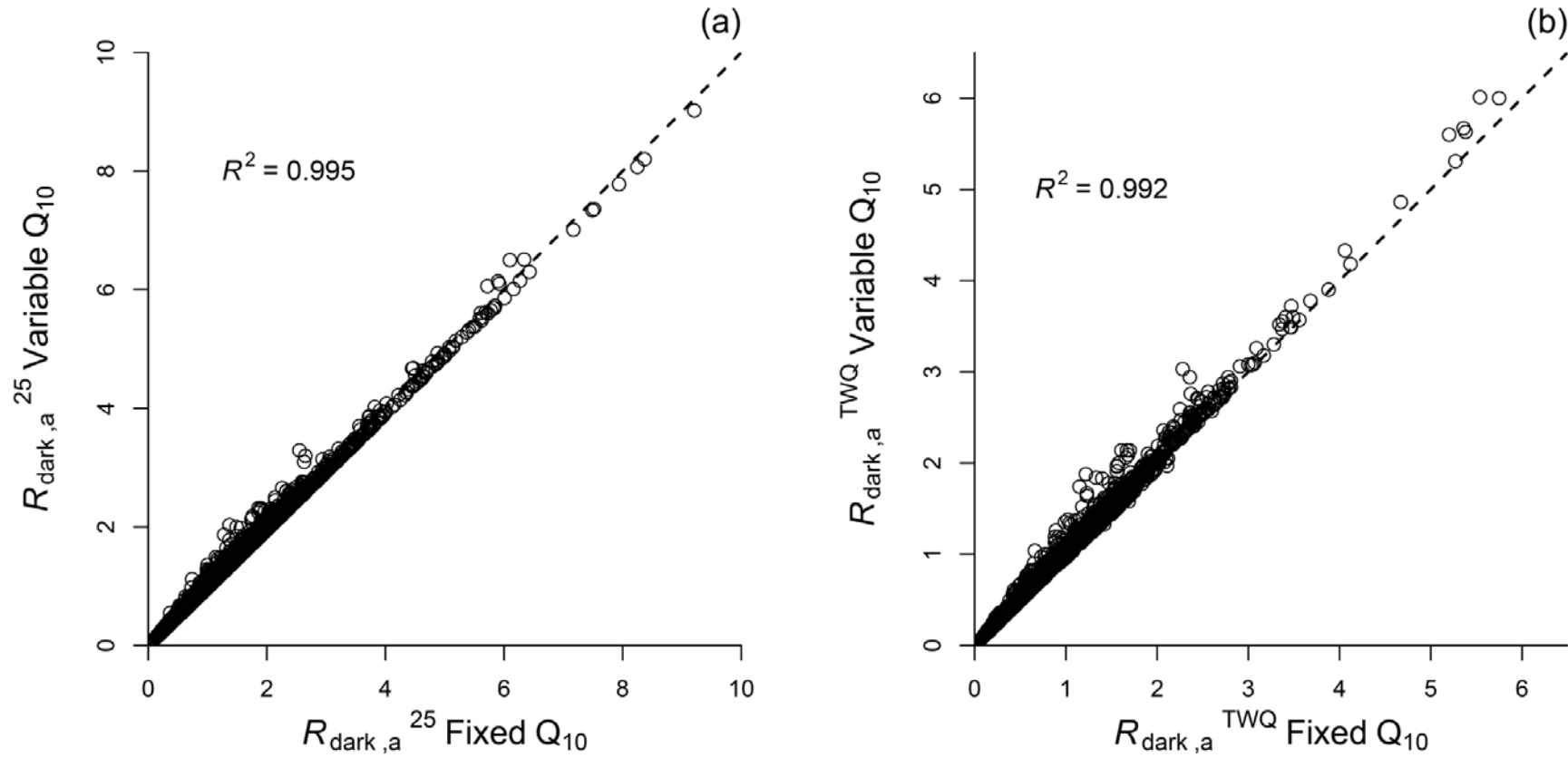
Fig. S1 Comparison of area-based rates of leaf respiration in darkness (R_{dark}) at a common leaf temperature of 25°C, calculated assuming either a fixed Q_{10} of 2.23 (Atkin *et al.*, 2005) (using Eqn 1 in the Materials and Methods section) or assuming a *T*-dependent Q_{10} (Tjoelker *et al.*, 2001) (using Eqn 2 Materials and Methods section). $R_{dark,a}^{25}$ and $R_{dark,a}^{TWQ}$, predicted area-based R_{dark} rates (μmol CO_2 m^{-2} s^{-1}) at 25°C, and TWQ (mean *T* of the warmest quarter), respectively. Values at the TWQ of each replicate were calculated using climate data from the *WorldClim* data base (Hijmans *et al.*, 2005). Data shown are for individual observational rows in the global respiration database.

Fig. S2 Relationships between leaf structural and chemical composition traits, and mean daily temperature of the warmest quarter (TWQ). Values shown are averages for unique site : species combinations in the global *GlobResp* database. Traits shown are: (a) M_a, leaf mass per unit leaf area; (b) $[N]_a$, area-based leaf nitrogen concentration; and (c) $[P]_a$, area-based leaf phosphorous concentration. TWQ at each site were obtained using site information and the *WorldClim* data base (Hijmans *et al.*, 2005). Solid grey line in each plot shows regression lines where the relationships were significant (with 95% confidence intervals shown as dashed line around the predicted relationship; the dotted lines show the prediction intervals (two-times the standard deviation) around the predicted relationship.
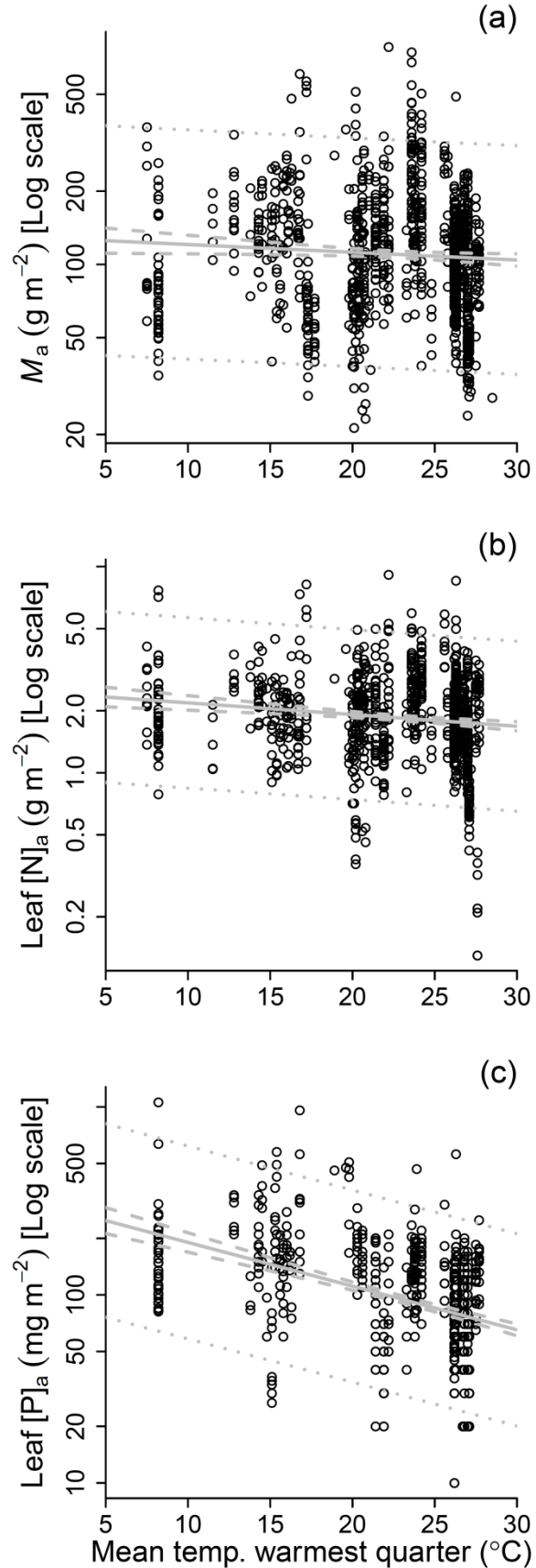
While the negative $M_a \leftrightarrow$ TWQ (a) and $[N]_a \leftrightarrow$ TWQ (Fig. 4b) relationships were both significant (M_a: $P < 0.05$, $n = 1092$; $[N]_a$: $P < 0.0001$, $n = 1029$), in neither case were the associations strong (M_a: Pearsons correlation (r) = -0.067, $r^2 = 0.004$; $[N]_a$: $r = -0.134$, $r^2 = 0.018$). By contrast, the negative $[P]_a \leftrightarrow$ TWQ relationship (Fig. 4c) was more marked ($P < 0.0001$, $n = 728$, $r = -0.418$, $r^2 = 0.174$), with $[P]_a$ being highest at the coldest sites.

Fig. S3 Site-species mean values leaf R_{dark} (log$_{10}$ scale) relationships with aridity index (AI), excluding data from the exceptionally high-rainfall, Frans Josef Glacier (FJG) site in New Zealand. Traits shown are: $R_{dark,a}^{25}$, (a) and $R_{dark,a}^{TWQ}$ (b), predicted area-based R_{dark} rates at 25°C and TWQ, respectively; $R_{dark,m}^{25}$ (c) and $R_{dark,m}^{TWQ}$ (d), predicted mass-based R_{dark} rates at 25°C and TWQ, respectively. Values at 25°C and TWQ were calculated assuming a temperature-dependent Q_{10} (Tjoelker *et al.*, 2001) and Equation 7 described in Atkin *et al.* (2005). Values at the TWQ of each replicate were calculated using climate/location data from the *WorldClim* data base (Hijmans *et al.*, 2005). Aridity index calculated as the ratio of mean annual precipitation (MAP) to mean annual potential evapotranspiration (PET) (UNEP, 1997). Solid lines in each plot show regression lines where the relationships were significant; dashed lines show the prediction intervals (two-times the SD) around the predicted relationship. See Fig. 4 for the same figure where data from FJG were included.
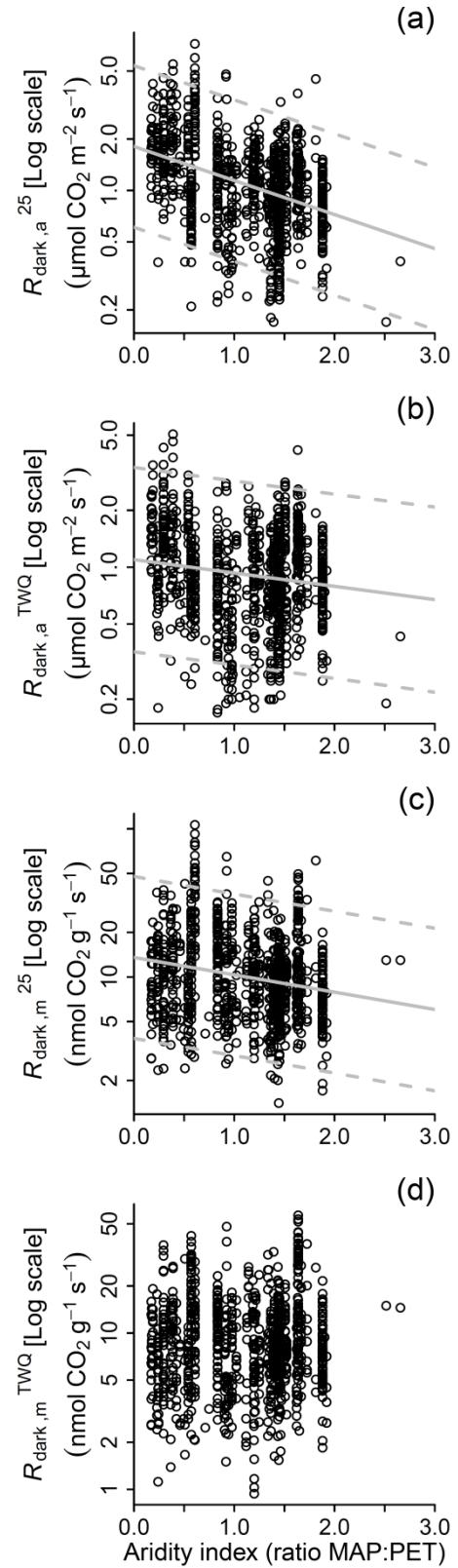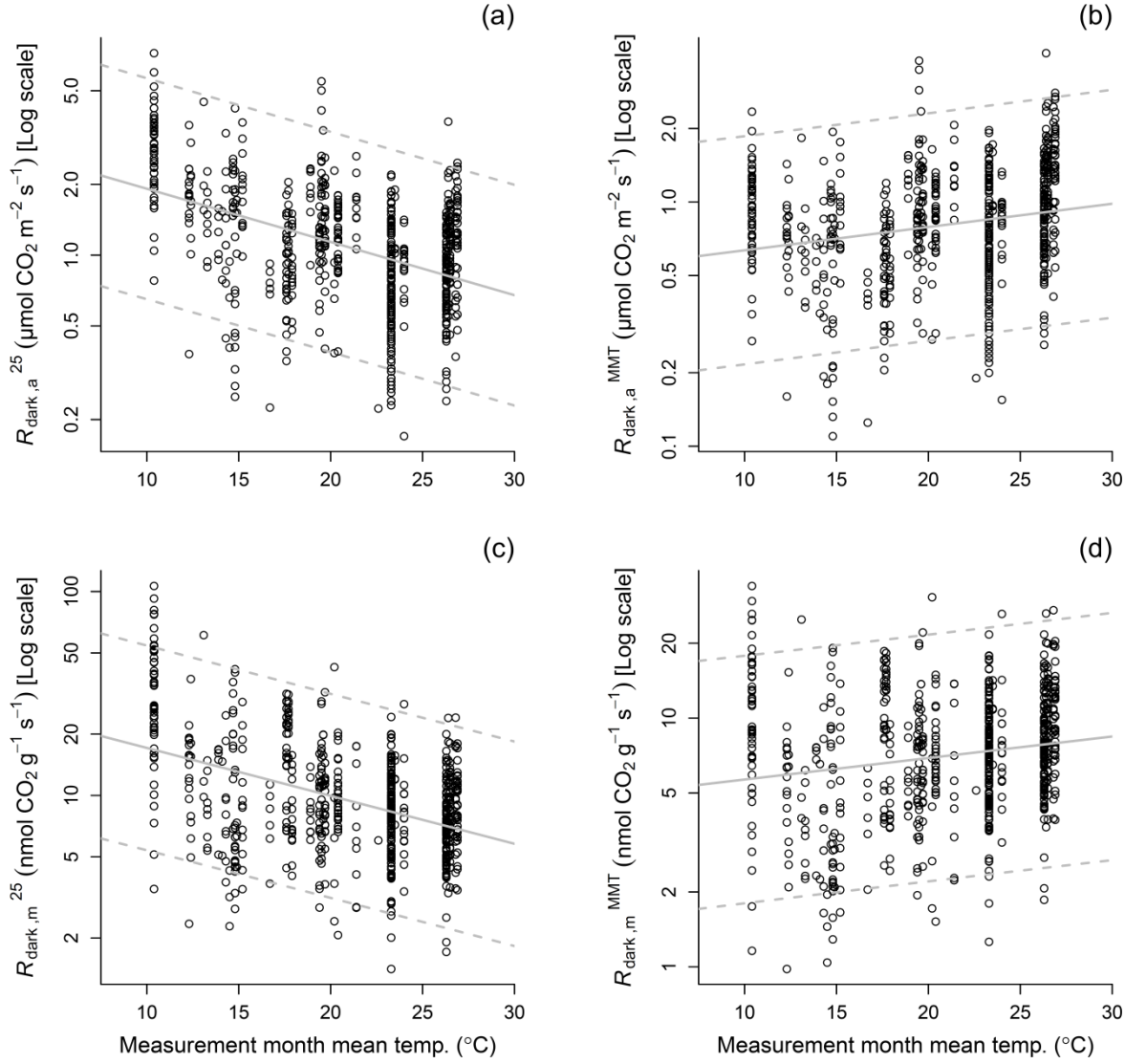
Fig. S4 Relationships between leaf R_{dark} (log$_{10}$ scale) and measuring month mean daily temperature (MMT) for those sites where the month of measurement was known. Values shown are averages for unique site : species combinations, using previously unpublished data (Table S1). Traits shown are: (a) $R_{dark,a}^{25}$, predicted area-based R_{dark} at 25°C; (b) $R_{dark,a}^{MMT}$, predicted area-based R_{dark} at MMT; (c) $R_{dark,m}^{25}$, mass-based R_{dark} at 25°C; (d) $R_{dark,m}^{MMT}$, mass-based R_{dark} at MMT. Values at 25°C and MMT were calculated assuming a T-dependent Q_{10} (Tjoelker *et al.*, 2001) and Equation 7 described in Atkin *et al.* (2005). Values at the MMT of each replicate were calculated using climate/location data from the *WorldClim* data base (Hijmans *et al.*, 2005). Solid lines in each plot show regression lines where the relationships were significant; dashed lines show the prediction intervals (two-times the standard deviation) around the predicted relationship. For $R_{dark,a}^{25}$, the negative relationship with MMT was significant ($P < 0.0001$, $n = 677$, $r^2 = 0.192$; log$_{10}$ $R_{dark,a}^{25} = 0.509 - 0.023 \times$ MMT) (a). Similarly, the $R_{dark,a}^{MMT} \leftrightarrow$ MMT association (b) was significant ($P < 0.0001$, $n = 677$, $r^2 = 0.041$; log$_{10}$ $R_{dark,a}^{MMT} = -0.293 + 0.0095 \times$ MMT), as were the $R_{dark,m}^{25} \leftrightarrow$ MMT ($P < 0.0001$, $n = 667$, $r^2 = 0.184$; log$_{10}$ $R_{dark,m}^{25} = 1.468 - 0.023 \times$ MMT) and $R_{dark,m}^{MMT} \leftrightarrow$ MMT ($P < 0.0001$, $n = 667$, $r^2 = 0.030$; log$_{10}$ $R_{dark,m}^{MMT} = 0.666 + 0.009 \times$ MMT) relationships (c, d).
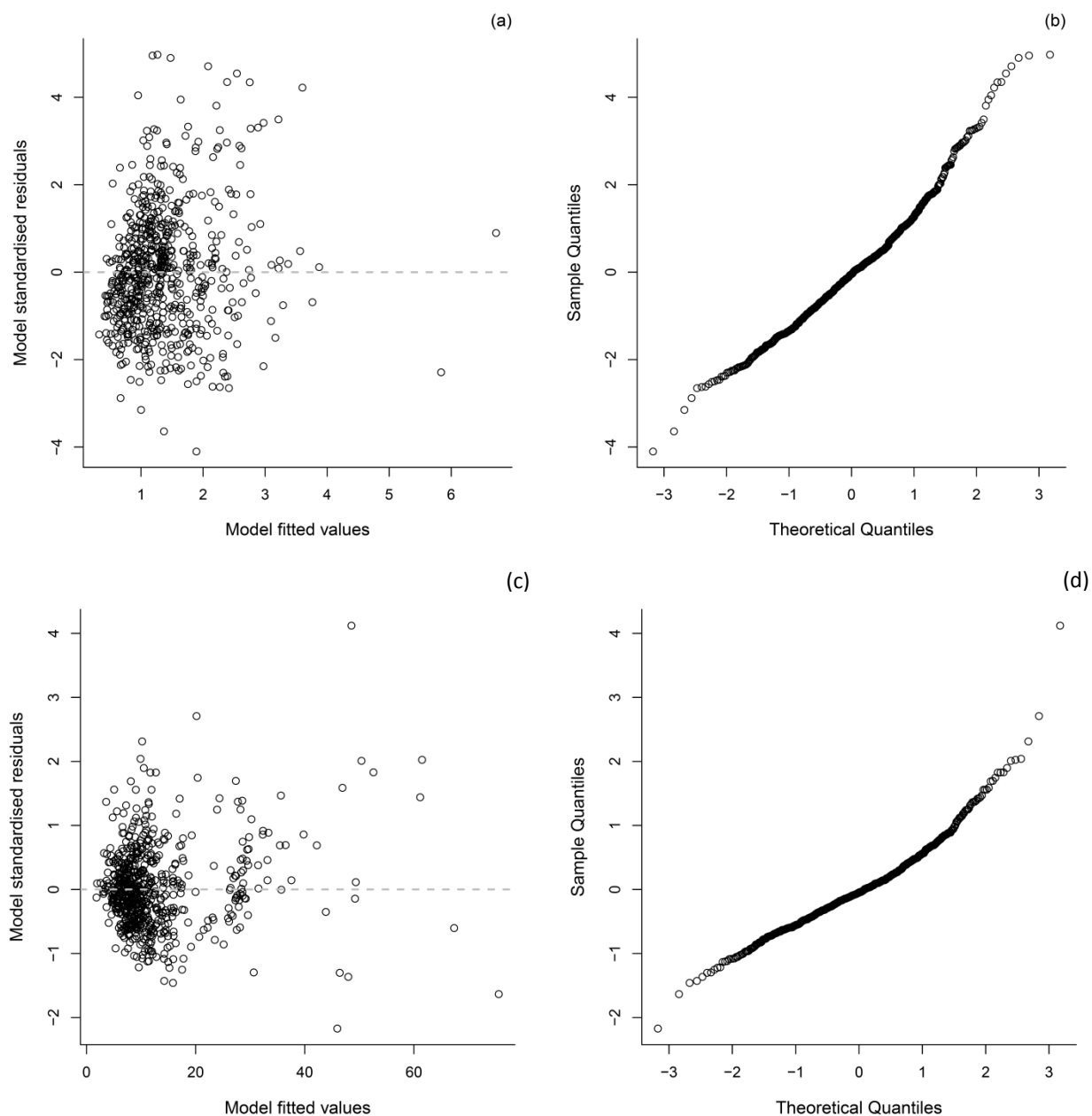
Fig. S5 Testing key assumptions for area- and mass-based mixed effects models – heterogeneity and normality. See Table 5 in the main text for details on the models. The upper panels (a, b) refer to the model based on area-based values, while the lower panels (c, d) refers to the mass-based model.
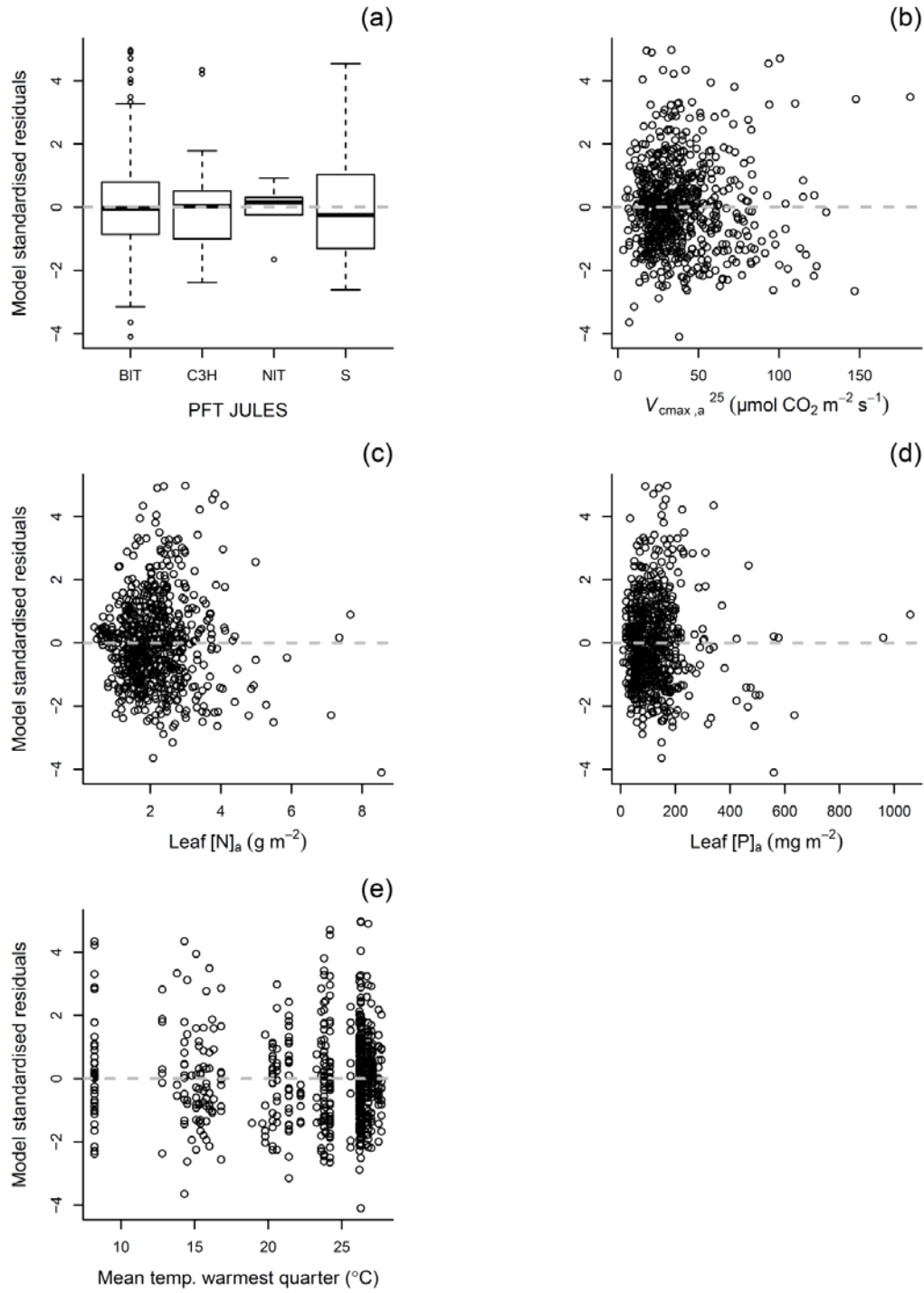
Fig. S6 Model validation graphs for the area-based mixed effects model. Shown are standardised residuals plotted against fitted values for each of the continuous explanatory factors and variables used in the model's fixed components: (a) plant functional types (PFT) categorised according to *JULES* (BlT, broadleaved trees; C3H, C_3 herbs; NlT, needle-leaved trees; S, shrubs); (b) area-based rates of the V_{cmax} of Rubisco at 25°C ($V_{cmax, a}^{25}$); (c) leaf nitrogen per unit leaf area ($[N]_a$); (d) leaf phosphorus per unit leaf area ($[P]_a$); and,(e) mean temperature of the warmest quarter at each site. See Table 5 for details on the models. Similar graphs were made for the mass-based model (data not shown). For (a), the central box in each plot shows the interquartile range; the median is shown as the bold line in each box; whiskers extend 1.5 times the interquartile range or the most extreme value, whichever is smaller; any points outside the values are shown as individual points.
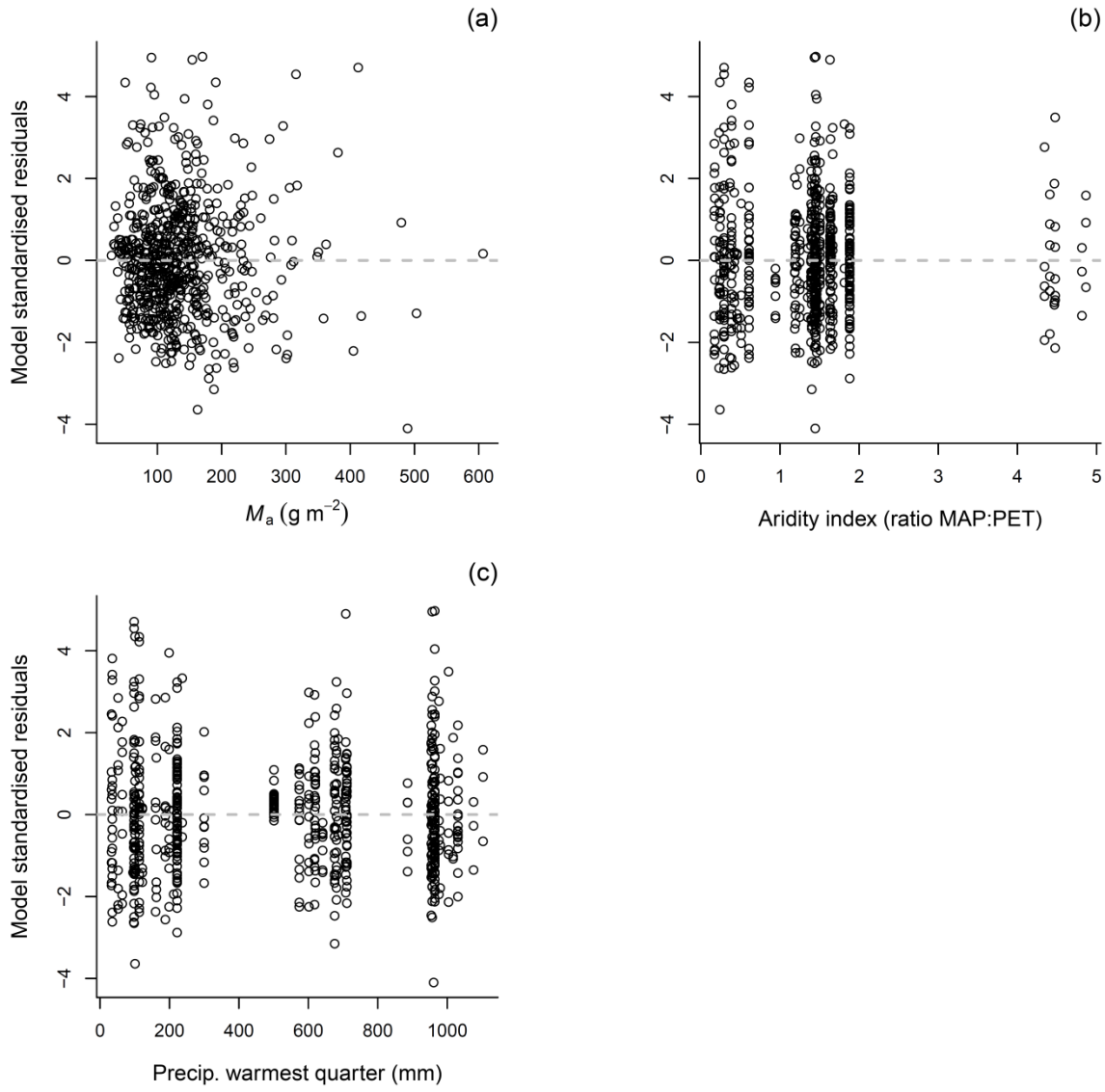
Fig. S7 Standardised residuals plotted against fitted values for variables *not* used in the area-based model's fixed components. See Table 5 for details on the models. Similar graphs were made for the mass-based model (data not shown). Plots show residuals against (a) leaf mass per unit leaf area (M_a) categorised; (b) aridity index (ratio of mean annual precipitation to potential evapotranspiration); (c) precipitation of the warmest quarter at each site.
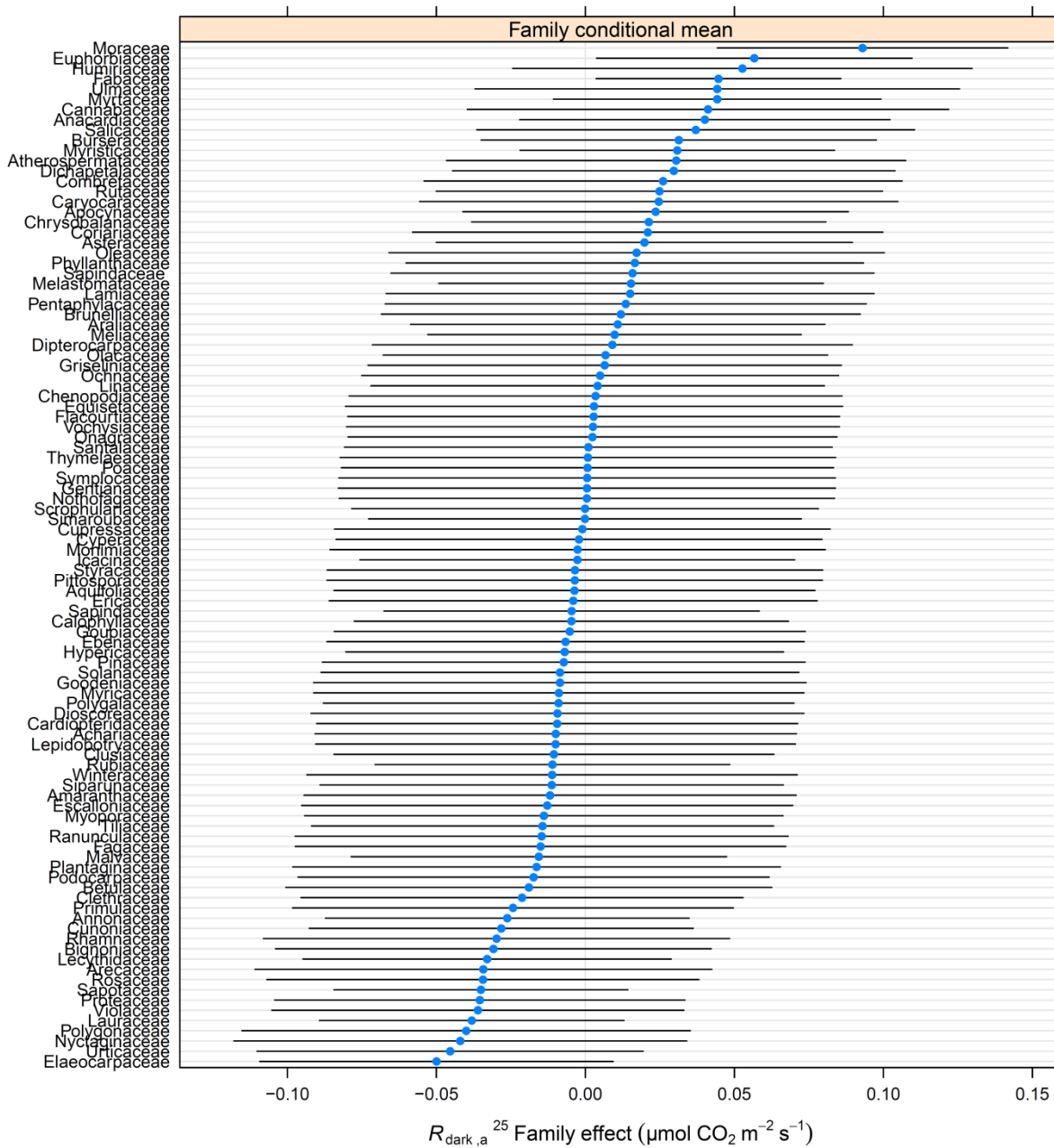
Fig. S8 Dotchart of the area-based mixed model's random intercepts by Family. Points represent the difference (shown with 95% prediction intervals) for each family in the $R_{dark,a}^{25}$ response above or below the overall population mean after controlling for the model's fixed terms and site location (Fig. S7). See Table 5 for details on the models. Similar graphs were made for the mass-based model (data not shown).
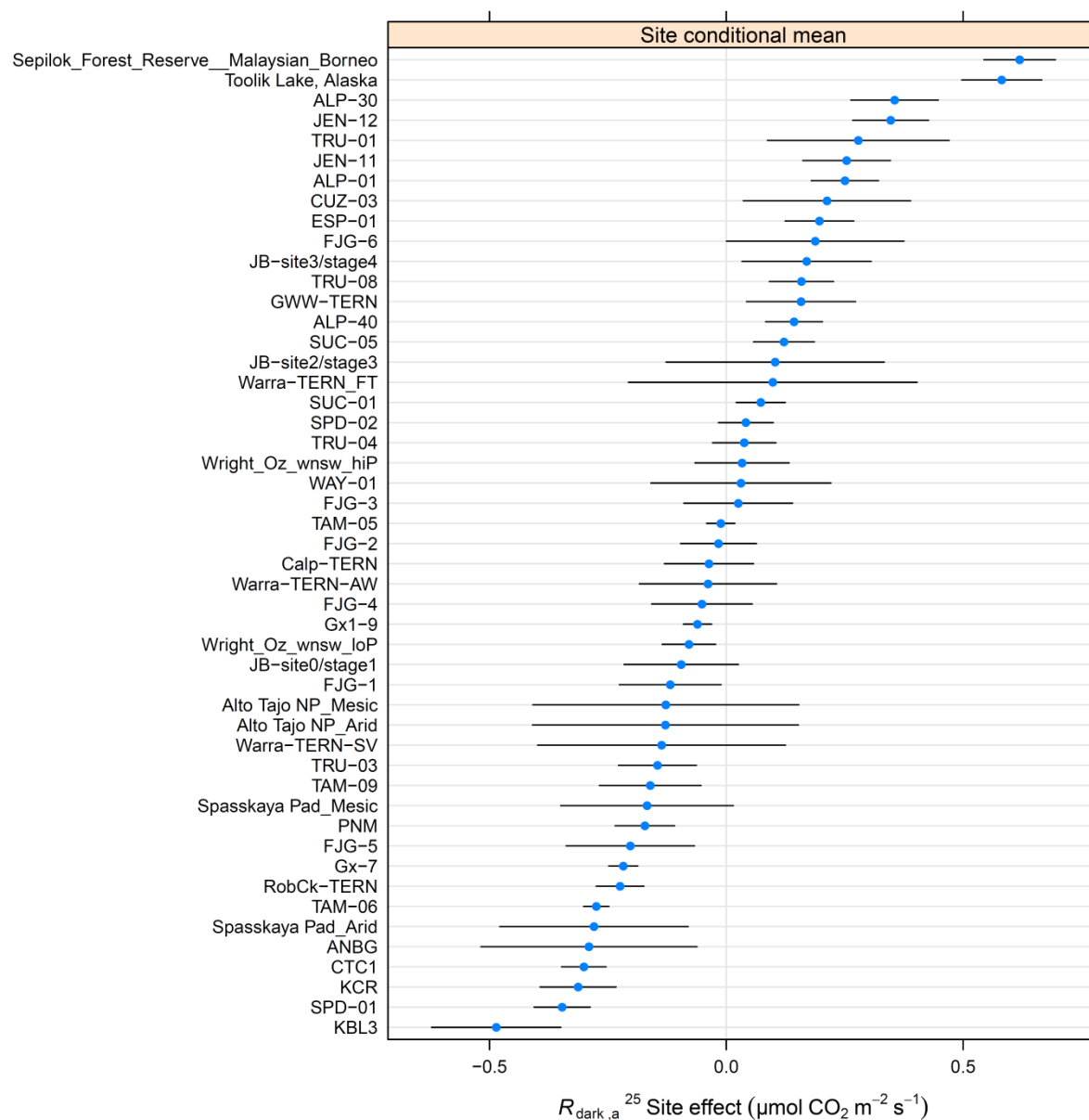
Fig. S9 Dotchart of the area-based mixed model's random intercepts by site. Points represent the difference (shown with 95% prediction intervals) for each site in the $R_{dark,a}^{25}$ response above or below the overall population mean after controlling for the model's fixed terms and phylogenetic structure (Fig. S6). See Table 5 for details on the models. Similar graphs were made for the mass-based model (data not shown)

References

Allen SE. 1974. *Chemical analysis of ecological materials*. Oxford, UK: Blackwell Scientific Publications.

Asner GP, Martin RE, Tupayachi R, Anderson CB, Sinca F, Carranza-Jiménez L, Martinez P. 2014. Amazonian functional diversity from forest canopy chemical assembly. *Proceedings of the National Academy of Sciences, USA* **111:** 5604–5609.

Atkin OK, Bruhn D, Tjoelker MG 2005. Response of plant respiration to changes in temperature: mechanisms and consequences of variations in Q_{10} values and acclimation. In: Lambers H, Ribas-Carbó M, eds. *Plant respiration: from cell to ecosystem*. Dordrecht, the Netherlands: Springer, 95–135.

Atkin OK, Evans JR, Siebke K. 1998. Relationship between the inhibition of leaf respiration by light and enhancement of leaf dark respiration following light treatment. *Australian Journal of Plant Physiology* **25:** 437–443.

Atkin OK, Tjoelker MG. 2003. Thermal acclimation and the dynamic response of plant respiration to temperature. *Trends in Plant Science* **8:** 343–351.

Atkin OK, Turnbull MH, Zaragoza-Castells J, Fyllas NM, Lloyd J, Meir P, Griffin KL. 2013. Light inhibition of leaf respiration as soil fertility declines along a post-glacial chronosequence in New Zealand: an analysis using the Kok method. *Plant and Soil* **367:** 163–182.

Azcón-Bieto J, Osmond CB. 1983. Relationship between photosynthesis and respiration. The effect of carbohydrate status on the rate of CO_2 production by respiration in darkened and illuminated wheat leaves. *Plant Physiology* **71:** 574–581.

Bolstad PV, Mitchell K, Vose JM. 1999. Foliar temperature-respiration response functions for broad-leaved tree species in the southern appalachians. *Tree Physiology* **19:** 871–878.

Chazdon RL, Kaufmann S. 1993. Plasticity of leaf anatomy of two rainforest shrubs in relation to photosynethetic light acclimation. *Functional Ecology* **7:** 385–394.

Clark DB, Mercado LM, Sitch S, Jones CD, Gedney N, Best MJ, Pryor M, Rooney GG, Essery RLH, Blyth E *et al*. **2011.** The Joint UK Land Environment Simulator (JULES), model description – Part 2: carbon fluxes and vegetation dynamics. *Geoscientific Model Development* **4:** 701–722.

Craine JM, Berin DM, Reich PB, Tilman GD, Knops JMH. 1999. Measurement of leaf longevity of 14 species of grasses and forbs using a novel approach. *New Phytologist* **142:** 475–481.

García-Núñez C, Azócar A, Rada F. 1995. Photosynthetic acclimation to light in juveniles of two cloud-forest tree species. *Trees – Structure and Function* **10:** 114–124.

Grueters U. 1998. *Der Kohlenstoffhaushalt von Weizen in der Interaktion erhöhter CO_2/O_3 Konzentrationen und Stickstoffversorgung*. PhD thesis, Justus-Liebig-University Giessen, Germany.

Heskel MA, Bitterman D, Atkin OK, Turnbull MH, Griffin KL. 2014. Seasonality of foliar respiration in two dominant plant species from the Arctic tundra: response to long-term warming and short-term temperature variability. *Functional Plant Biology* **41:** 287–300.

Hijmans RJ, Cameron SE, Parra JL, Jones PG, Jarvis A. 2005. Very high resolution interpolated climate surfaces for global land areas. *International Journal of Climatology* **25:** 1965–1978.

Kamaluddin M, Grace J. 1993. Growth and photosynthesis of tropical forest tree seedlings (*Bischofia javanica* Blume) as influenced by a change in light availability. *Tree Physiology* **13:** 189–201.

Kattge J, Díaz S, Lavorel S, Prentice IC, Leadley P, Bönisch G, Garnier E, Westoby M, Reich PB, Wright IJ *et al.* 2011. TRY – a global database of plant traits. *Global Change Biology* **17:** 2905–2935.

Kitajima K, Mulkey SS, Wright SJ. 1997. Seasonal leaf phenotypes in the canopy of a tropical dry forest: photosynthetic characteristics and associated traits. *Oecologia* **109:** 490–498.

Kloeppel BD, Abrams MD. 1995. Ecophysiological attributes of the native *Acer saccharum* and the exotic *Acer platanoides* in urban oak forests in Pennsylvania, USA. *Tree Physiology* **15:** 739–746.

Kloeppel BD, Abrams MD, Kubiske ME. 1993. Seasonal ecophysiology and leaf morphology of four successional Pennsylvania barrens species in open versus understory environments. *Canadian Journal of Forest Research* **23:** 181–189.

Kloeppel BD, Kubiske ME, Abrams MD. 1994. Seasonal tissue water relations of four successional Pennsylvania barrens species in open and understory environments. *International Journal of Plant Sciences* **155:** 73–79.

Kok B. 1948. A critical consideration of the quantum yield of *Chlorella*-photosynthesis. *Enzymologia* **13:** 1–56.

Lee TD, Reich PB, Bolstad PV. 2005. Acclimation of leaf respiration to temperature is rapid and related to specific leaf area, soluble sugars and leaf nitrogen across three temperate deciduous tree species. *Functional Ecology* **19:** 640–647.

Lopez-Gonzalez G, Lewis SL, Burkitt M, Phillips OL. 2011. ForestPlots.net: a web application and research tool to manage and analyse tropical forest plot data. *Journal of Vegetation Science* **22:** 610–613.

Lusk CH, Reich PB. 2000. Relationships of leaf dark respiration with light environment and tissue nitrogen content in juveniles of 11 cold-temperate tree species. *Oecologia* **123:** 318–329.

Machado JL, Reich PB. 2006. Dark respiration rate increases with plant size in saplings of three temperate tree species despite decreasing tissue nitrogen and nonstructural carbohydrates. *Tree Physiology* **26:** 915–923.

Meir P, Kruijt B, Broadmeadow M, Barbosa E, Kull O, Carswell F, Nobre A, Jarvis PG. 2002. Acclimation of photosynthetic capacity to irradiance in tree canopies in relation to leaf nitrogen concentration and leaf mass per unit area. *Plant, Cell & Environment* **25:** 343–357.

Meir P, Levy PE, Grace J, Jarvis PG. 2007. Photosynthetic parameters from two contrasting woody vegetation types in West Africa. *Plant Ecology* **192:** 277–287.

Mitchell KA, Bolstad PV, Vose JM. 1999. Interspecific and environmentally induced variation in foliar dark respiration among eighteen southeastern deciduous tree species. *Tree Physiology* **19:** 861–870.

Miyazawa S, Satomi S, Terashima I. 1998. Slow leaf development of evergreen broad-leaved tree species in Japanese warm temperate forests. *Annals of Botany* **82:** 859–869.

Mooney HA, Field C, Gulmon SL, Rundel P, Kruger FJ. 1983. Photosynthetic characteristic of South African sclerophylls. *Oecologia* **58:** 398–401.

Oberbauer SF, Strain BR. 1985. Effects of light regime on the growth and physiology of *Pentaclethra macroloba* (Mimosaceae) in Costa Rica. *Journal of Tropical Ecology* **1:** 303–320.

Oberbauer SF, Strain BR. 1986. Effects of canopy position and irradiance on the leaf physiology and morphology of *Pentaclethra macroloba* (Mimosaceae). *American Journal of Botany* **73:** 409–416.

Poorter L, Bongers F. 2006. Leaf traits are good predictors of plant performance across 53 rain forest species. *Ecology* **87:** 1733–1743.

Reich PB, Ellsworth DS, Walters MB. 1998a. Leaf structure (specific leaf area) modulates photosynthesis-nitrogen relations: evidence from within and across species and functional groups. *Functional Ecology* **12:** 948–958.

Reich PB, Ellsworth DS, Walters MB, Vose JM, Gresham C, Volin JC, Bowman WD. 1999. Generality of leaf trait relationships: a test across six biomes. *Ecology* **80:** 1955–1969.

Reich PB, Tjoelker MG, Pregitzer KS, Wright IJ, Oleksyn J, Machado JL. 2008. Scaling of respiration to nitrogen in leaves, stems and roots of higher land plants. *Ecology Letters* **11:** 793–801.

Reich PB, Walters MB, Ellsworth DS, Vose JM, Volin JC, Gresham C, Bowman WD. 1998b. Relationships of leaf dark respiration to leaf nitrogen, specific leaf area and leaf life-span: a test across biomes and functional groups. *Oecologia* **114:** 471–482.

Schulze ED, Kelliher FM, Körner C, Lloyd J, Leuning R. 1994. Relationships among maximum stomatal conductance, ecosystem surface conductance, carbon assimilation rate, and plant nitrogen nutrition – a global ecology scaling exercise. *Annual Review of Ecology and Systematics* **25:** 629–660.

Sendall KM, Reich PB. 2013. Variation in leaf and twig CO_2 flux as a function of plant size: a comparison of seedlings, saplings and trees. *Tree Physiology* **33:** 713–729.

Sitch S, Smith B, Prentice IC, Arneth A, Bondeau A, Cramer W, Kaplan JO, Levis S, Lucht W, Sykes MT *et al*. 2003. Evaluation of ecosystem dynamics, plant geography and terrestrial carbon cycling in the LPJ dynamic global vegetation model. *Global Change Biology* **9:** 161–185.

Slot M, Rey-Sánchez C, Winter K, Kitajima K. 2014. Trait-based scaling of temperature-dependent foliar respiration in a species-rich tropical forest canopy. *Functional Ecology* **28:** 1074–1086.

Swaine EK. 2007. *Ecological and evolutionary drivers of plant community assembly in a Bornean rain forest.* Aberdeen, UK: University of Aberdeen.

Tjoelker MG, Craine JM, Wedin D, Reich PB, Tilman D. 2005. Linking leaf and root trait syndromes among 39 grassland and savannah species. *New Phytologist* **167:** 493–508.

Tjoelker MG, Oleksyn J, Reich PB. 2001. Modelling respiration of vegetation: evidence for a general temperature-dependent Q_{10}. *Global Change Biology* **7:** 223–230.

Tjoelker MG, Oleksyn J, Reich PB, Zytkowiak R. 2008. Coupling of respiration, nitrogen, and sugars underlies convergent temperature acclimation in *Pinus banksiana* across wide-ranging sites and populations. *Global Change Biology* **14:** 782–797.

UNEP. 1997. *World atlas of desertification*. London, UK: United Nations Environment Programme.

Weerasinghe LK, Creek D, Crous KY, Xiang S, Liddell MJ, Turnbull MH, Atkin OK. 2014. Canopy position affects the relationships between leaf respiration and associated traits in a tropical rainforest in Far North Queensland. *Tree Physiology* **34:** 564–584.

Wright IJ, Reich PB, Atkin OK, Lusk CH, Tjoelker MG, Westoby M. 2006. Irradiance, temperature and rainfall influence leaf dark respiration in woody plants: evidence from comparisons across 20 sites. *New Phytologist* **169:** 309–319.

Wright IJ, Reich PB, Westoby M. 2001. Strategy shifts in leaf physiology, structure and nutrient content between species of high- and low-rainfall and high- and low-nutrient habitats. *Functional Ecology* **15:** 423–434.

Wright IJ, Reich PB, Westoby M, Ackerly DD, Baruch Z, Bongers F, Cavender-Bares J, Chapin T, Cornelissen JHC, Diemer M *et al*. 2004. The worldwide leaf economics spectrum. *Nature* **428:** 821–827.

Zotz G, Winter K. 1996. Diel patterns of CO_2 exchange in rainforest canopy plants. In: Mulkey SS, Chazdon RL, Smith AP, eds. *Tropical forest plant ecophysiology*. New York, NY, USA: Chapman & Hall, 89–113.